NASA TN D-1574

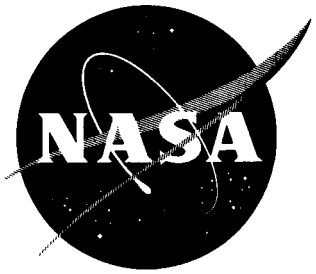

TECHNICAL NOTE

D-1574

FATIGUE BEHAVIOR OF MATERIALS UNDER STRAIN CYCLING IN LOW AND INTERMEDIATE LIFE RANGE

By Robert W. Smith, Marvin H. Hirschberg, and S. S. Manson

Lewis Research Center
Cleveland, Ohio

NATIONAL AERONAUTICS AND SPACE ADMINISTRATION
WASHINGTON
April 1963

NATIONAL AERONAUTICS AND SPACE ADMINISTRATION

TECHNICAL NOTE D-1574

FATIGUE BEHAVIOR OF MATERIALS UNDER STRAIN CYCLING IN LOW AND INTERMEDIATE LIFE RANGE

By Robert W. Smith, Marvin H. Hirschberg, and S. S. Manson

SUMMARY

A series of constant strain range tests was made for a wide variety of materials producing fatigue lives varying from a few cycles to about one million cycles. The specimens were subjected to axial, compression-tension, low-frequency fatigue about a zero mean strain. Load range was measured periodically throughout each test, enabling an analysis of fatigue results in terms of elastic, plastic, and total strains. Materials tested were AISI 4130 (soft and hard), AISI 4340 (annealed and hard), AISI 52100, AISI 304 ELC (annealed and hard), AISI 310 (annealed), AM 350 (annealed and hard), Inconel X, titanium (6Al-4V), 2014-T6, 5456-H311, and 1100 aluminum, and beryllium.

During strain cycling, load range generally changes during the very early part of the test and then settles down to a fairly constant value for most of the fatigue life. Cyclic strain hardening or softening causes the observed load change and produces cyclic stress-strain relations that often differ substantially from the virgin tensile flow curve. These comparisons are made for each of the test materials.

Fatigue-life relations between elastic, plastic, and total strain components were established. For metallurgically stable materials, straight-line fits of the logarithmic elastic strain-life and plastic strain-life data produce a relation that agrees well with the total strain-life data. The strain-life data are also used to explain changes in susceptibility to stress concentrations over a large life span and to rate correctly the relative notch sensitivities of the four test materials that experienced nontest-section failures in comparison with the other materials.

Relative performance of the test materials is illustrated on the basis of both strain range and stress range over a life span ranging from a few cycles to about one million cycles.

INTRODUCTION

In recent years there has been an appreciable effort to incorporate low-cycle fatigue data obtained at various laboratories into fatigue design procedures. Manson (ref. 1) and Coffin (ref. 2) independently suggested that low-cycle fatigue life for a specific material is directly proportional to a power of the cyclic plastic strain (a straight line on a log-log plot of plastic strain against cycles to failure). Coffin (ref. 3) discussed the application of this criterion to design after extensive testing of type 347 stainless steel in both constrained thermal cycling and constant-temperature strain cycling. Correlated experimental data were developed at four laboratories to establish parameters governing pressure-vessel design with respect to the plastic fatigue characteristics of the material (ref. 4). In this analysis use was made of total (elastic plus plastic) strain range test data. Manson (ref. 5) has related fatigue life to the elastic as well as the plastic strain range components of the total mechanical strain range, thereby producing one relation suitable for cyclic lives of approximately 10 to 10^6 cycles. It has also been pointed out (ref. 6) that in elastic-plastic stress analysis of fatigue problems there is a definite need for knowledge of the relation between stress range (or amplitude) and strain range (or amplitude) during strain cycling. Most recently, Langer (ref. 7) has described a pressure-vessel design procedure using a stress amplitude-life equation based on two factors: an empirical relation between plastic strain and tensile ductility, and the endurance limit.

In order to evaluate present design procedures, to develop new methods if necessary, and to increase the understanding of the stress-strain - life relations during fatigue, it was believed desirable to obtain detailed fatigue test data for a wide variety of ductile materials using axial, compression-tension, low-frequency fatigue machines in which both load and deformation were measured periodically throughout the test. The first phase of such a program, reported herein, provides the basic information obtained from room-temperature constant diametral strain range tests with zero mean strain. The following desired test information was obtained:

(1) Behavior of load range during cycling at constant strain amplitude

(2) Fatigue behavior for span of fatigue life ranging from a few cycles to about one million cycles

(3) Data for a selection of materials in which there is a wide variation of chemical and metallurgical composition

(4) Data for a selection of materials in which there is a wide variation in elastic and mechanical properties (elastic modulus, yield strength, ultimate strength, and ductility)

Such information is then used to

(1) Determine the cyclic stress-strain relations necessary to the stress analyst for fatigue analysis

(2) Determine the elastic strain (or stress), the plastic strain, and the total strain range as a function of fatigue life

(3) Compare relative performance of materials on a basis of strain range and stress range

(4) Illustrate the use of strain-life relations to indicate relative notch sensitivity of the materials

MATERIALS, APPARATUS, AND PROCEDURE

Materials Tested

The nominal chemical composition, processing condition, and hardness of each test material are tabulated in table I. The test materials were three ferritic alloy steels: AISI 4130, AISI 4340, and AISI 52100; three austenitic heat-resisting steels: AISI 304 (extra low carbon), AISI 310, and AM 350; one heat-resisting nickel-base alloy: Inconel X; three types of aluminum: 2014-T6, 5456-H311, and 1100; a 6Al-4V titanium alloy; and structural grade QMV beryllium. The steels AISI 4130, 4340, and 304 ELC, and AM 350 were tested in both soft and hard conditions. Mechanical properties for these materials (table II) were measured at room temperature.

Specimen Configuration

The fatigue test specimens (figs. 1(a) and (b)) were bars, circular in cross section having an hourglass-shaped test section with a minimum diameter of 0.25 inch, unless otherwise noted in table III. AISI 4130 and 52100 steels were fabricated from 1/2-inch-diameter blanks into fatigue specimens as shown in figure 1(b). All the rest of the materials were machined out of 3/4-inch-diameter blanks into buttonhead fatigue specimens as shown in figure 1(a) (or fig. 1(c) for beryllium only). Separate buttonheads were screwed onto the threaded-head specimens so that the same style of grips could be used for all materials. It was necessary to use a modified specimen configuration for certain very short life tests to reduce the buckling problem that developed in the more ductile materials at large diametral strain ranges. The most common modification involved the reduction of the hourglass radius to 1.0 inch and the overall specimen length to 2.25 inches. In a few tests of AISI 4130 (annealed and hard) and Inconel X the hourglass radius was further reduced to 0.5 inch. Another modification was necessary to prevent failures outside the test section for some materials under certain test conditions. In this case the minimum test-section diameter was reduced to 0.21 or 0.18 inch as circumstances dictated.

A cylindrical test section (fig. 1(c)) was used to make the longitudinal strain measurements necessary for elastic modulus determinations. Beryllium fatigue specimens were made of this configuration also to allow longitudinal strain control instead of diametral. This procedure was necessary because the extremely

low value of Poisson's ratio (μ = 0.024) for beryllium means that the elastic diametrical strains are very small and, therefore, more difficult to measure accurately.

Test Apparatus

Four low-frequency mechanical fatigue testing machines (fig. 2) designed and built at Lewis Research Center were used for this test program. Alternate push and pull forces on the specimen were supplied by a 6-inch-diameter hydraulic cylinder. The buttonhead specimens were attached rigidly to the loading rods with split-cone and wedge-type grips. A commercial die set was used to maintain alinement under the action of compressive loads. The lower loading rod was attached in series to the lower movable die-set platen, the commercial load cell, and the hydraulically operated piston rod.

Strain range control was obtained by a 10-to-1 deflection lever attached to the moving platen. This lever actuated microswitches which energized relays that control a solenoid-operated four-way hydraulic valve. The valve transferred high-pressure oil to the opposite side of the double-acting piston and vented the unpressurized side to the supply tank. Cycling rate could be varied from as low as 2 or 3 cycles per minute to about 30 cycles per minute.

A strip-chart recorder was used to make either continuous or periodic records of load amplitude. A special circuit built into the recorder for this purpose powered the load cell which, in turn, supplied the load signals to the recorder for amplification.

Strain measurements were made with Tuckerman optical strain gages for all tests in which the diametral strain range fell below the maximum practical capability (ϵ^d = 0.034 in./in. or less) of the 1-inch-gage-length extensometer. (Symbols are defined in appendix A.) For larger strain ranges, a dial indicator type of diametral extensometer was used. Tuckerman optical strain gages were selected because of their reliability for a practically unlimited number of cycles at large as well as small strains, and because their excellent sensitivity is particularly desirable for diametral strain measurements. With these gages it is possible to discern a strain of 8 microinches per inch over a 1/4-inch gage length. Diametral strain measurements were made using two 1-inch extensometers fastened with piano-wire springs to a special diametral strain-gage fixture (figs. 3(a) and (b)). Two diametrically opposed aluminum bearing edges were rigidly fastened to a U-shaped leaf spring which pressed the bearing edges against the test section. Long flexible loops of piano wire attached to the loading rod stabilized the strain-gage fixture against tipping during the fatigue test. Longitudinal strain measurements, used for the beryllium fatigue tests and for all elastic modulus measurements, were made by fastening two 1-inch-gage-length extensometers directly to specimens having cylindrical test sections. All optical strain readings were made with the use of the Tuckerman autocollimators.

Procedure

Determination of mechanical properties. - The usual procedure involved the measurement of tensile and elastic properties before fatigue testing each test material. For tensile testing, standard hourglass fatigue specimens were installed in a Rhiele universal testing machine and were fitted with a dial-gage-type diametral extensometer. As the tensile load was increased, simultaneous readings of the dial gage and load indicator were recorded. With these data the true stress - true strain relation beyond the yield point was established. Other quantities measured and used to calculate ultimate strength, fracture strength, and ductility were maximum load, fracture load, and the minimum test-section diameter after fracture. In all cases the reported tensile properties (table II) represent the average of at least three tests. Cylindrical test-section specimens (fig. 1(c)) were used to determine elastic modulus and Poisson's ratio. Two 1-inch-gage-length optical extensometers were attached in the axial direction to opposite sides of the test section for strain measurement. Simultaneous strain and load readings taken at regular increments of both increasing and decreasing load provided the information necessary to plot the stress-strain curve from which the elastic modulus was determined by averaging the slope of the straight-line portions of this curve. The optical strain gages were then removed from the test section and replaced with the specially designed diametral strain-gage fixture for use with optical gages (fig. 3). A similar series of simultaneous load and diametral-strain readings was used to plot this relation. The slope of the straight-line portions of this curve represents the ratio E/μ, so that Poisson's ratio μ can be established from this slope and the previously calculated elastic modulus E. The values of E and μ (table II) were rounded off to two significant figures.

Fatigue testing. - The fatigue machine was operated manually during the first few cycles of each test to set the platen displacement limit switches (fig. 2) to produce the desired diametral strain range $\Delta\epsilon^d$ as measured at the test section. Initial loading was chosen to be compressive rather than tensile, because it was much easier to stop deformation of the test section at the desired strain level by manipulation of the pressure regulator. The natural increase of cross-sectional area during compressive flow reduces the required sensitivity of initial load control, whereas the reduction of area associated with tensile deformations increases the required sensitivity. Also, the initial plastic flow in compression tends to reduce the subsequent sharpness of the "knee" of the virgin stress-strain curve, which makes the control of tensile strains easier. The specimen was first compressed to produce an increase in strain of an amount $\frac{1}{2}\Delta\epsilon^d$ by slowly increasing the oil pressure to the hydraulic cylinder. When this strain was reached, the compression microswitch was set to be tripped by the deflection lever. The compression load was removed, and tension was slowly applied to produce a diametral decrease of strain of $\frac{1}{2}\Delta\epsilon^d$ from the initial diameter. When this strain was reached, the tension microswitch was adjusted. Thus, the specimen was strain cycled about a zero mean strain over a strain range of $\Delta\epsilon^d$.

Automatic operation of the fatigue machine was begun once the limit switches had been positioned so that the deflection lever triggered the switches at the desired strain limits as observed with the optical strain gages. Repeated checks were made of strain range throughout the test. Strain softening or strain hardening of the test specimens necessitated minor adjustments in the deflection-lever limit-switch settings in order to maintain constant $\Delta\epsilon^d$. These adjustments were necessary because the limit switches maintained constant displacement between upper and lower die-set platens. The loading rods, grips, and specimen heads were subjected to deflections entirely within the elastic range, but the test section of the specimen flowed plastically, undergoing a gradual change in material properties. Hence, as the test progressed, there was a change in strain distribution; and, in order to maintain a constant strain range at the test section, it was necessary to change the displacement limits between the platens. For a strain-hardening material these limits had to be increased, and for a strain-softening material they had to be decreased. Microswitch adjustments were made whenever the diametral strain range deviated 40 to 80 microinches from the desired value.

Continuous load recordings were taken during the early part of every test. Periodic load measurements were taken thereafter throughout the test in conjunction with the strain measurements. The basic test information periodically recorded throughout each test comprised total diametral strain range $\Delta\epsilon^d$, load range ΔP, and number of cycles N. Specimen life was defined as the number of cycles causing separation of the test section.

Special precautions, described in appendix B, were taken while testing beryllium to prevent distribution of toxic beryllium dust particles into the air.

RESULTS AND DISCUSSION

The basic test data, descriptive test information, and calculated stresses and strains are tabulated in table III for each fatigue test. Equations used to calculate these various quantities will be discussed later. Information from this table was used to plot most of the curves used in the subsequent analysis.

Cyclic Stress-Strain Relation

When fatigue specimens are cycled between fixed strain limits, the stress range generally changes during the test. Figure 4 shows the typical variations of stress range $\Delta\sigma = \Delta P/A$ with cycles for each of the test materials at three different values of applied strain range (zero mean strain in all cases). One group of materials including the heat-treatable ferritic alloy steels (figs. 4(a) to (e)), hardened AM 350 stainless (fig. 4(j)), and titanium (6Al-4V) (fig. 4(l)) is characterized by a stress range that decreases from the initial value. Since the stress required to produce a fixed strain decreases in successive cycles, and since hardness tests indicate a coincident softening, these materials are described as cyclic strain softening. A second group of materials

including stainless steels (figs. 4(f) to (i)), Inconel X (fig. 4(k)), 5456-H311 aluminum (fig. 4(n)), and beryllium (fig. 4(p)) shows an increase of stress and hardness during strain cycling. These are therefore called cyclic strain-hardening materials. Commercial purity 1100 aluminum (fig. 4(o)) displays a decrease in stress range with life, but this change is not simply a result of strain softening. Visible macrocracks that appear very early in these test specimens cause a reduction in stress range because the load-carrying ability in the tensile portion of the strain cycle is reduced. Little change in stress range takes place for 2014-T6 aluminum for the strain ranges shown in figure 4(m).

In addition to illustrating the strain-hardening and strain-softening characteristics, these figures indicate that the most significant changes in stress range usually occur within the first 20 percent of specimen life. During the remaining 80 percent or more of the life, the stress range remains relatively constant. This latter value of stress range can be considered then as a characteristic value corresponding to the applied range. For the purposes of subsequent analysis the stress range $\Delta\sigma$ at one-half the number of cycles to failure $\frac{1}{2} N_f$ was selected as the characteristic value.

The stress analyst who wishes to calculate the stress and strain distribution during fatigue involving plastic flow needs to know the characteristic stress range corresponding to an applied strain range. If the material undergoes cyclic strain softening or hardening, then he cannot properly use the tensile stress-strain relation of the virgin material, but he needs instead the stress-strain curve that applies following shakedown in fatigue. (Shakedown is defined herein as the condition that develops after a sufficient number of cycles have been applied to "stabilize" the stress range. Changes in stress range in successive cycles after shakedown are relatively small compared with those in the early cycles of strain.) Such a curve is established from fatigue test data by plotting the stress amplitude at shakedown in fatigue against the accompanying longitudinal total strain amplitude. Figure 5 graphically illustrates the difference between these two stress-strain relations and a method by which the desired relation can be obtained. Consider, for example, a test for which the strain amplitude is 0.018 inch per inch, corresponding to point A in figure 5(a). During the first quarter cycle, the stress amplitude will be governed by the static stress-strain curve, which indicates a required stress amplitude of 120 ksi. This stress is transferred to point A' of figure 5(b) in which stress amplitude is plotted against number of cycles. As the strain amplitude of 0.018 is repetitively applied, the stress amplitude increases and then levels off at 140 ksi as indicated by curve $A'P_A N_f$. Point A" (fig. 5(a)), representing the applied strain amplitude (0.018 in./in.) and the stress range at $\frac{1}{2} N_f$ (140 ksi), is then one point on the desired cyclic stress-strain curve. A similar point B" is obtained from another test of strain amplitude (0.036 in./in.); A" and B" represent two points on the cyclic stress-strain curve which is fully obtained from a series of different constant-strain range tests.

Data necessary to plot the cyclic stress-strain curve (in terms of stress amplitude σ_a against longitudinal strain amplitude ϵ_a^l) are readily calculated using the applied diametral strain range $\Delta\epsilon^d$ and the stress range $\Delta\sigma$ at $\frac{1}{2} N_f$. It was observed during zero mean strain fatigue testing that the maximum compressive and tensile stresses during any one cycle remained approximately equal to one another throughout the test. In other words, cyclic strain hardening or softening affected the peak tensile or compressive stresses equally, and the mean stress throughout a test was zero. By definition

$$\sigma_a = \frac{\Delta\sigma}{2} = \frac{\Delta P}{2A} \tag{1}$$

where

ΔP applied load range at $\frac{1}{2} N_f$

A cross-sectional area

Total mechanical strain amplitudes ϵ_a^l and ϵ_a^d are equal to the sum of the elastic and plastic strain components when creep and anelastic strains are negligible. Thus,

$$\epsilon_a^l = \epsilon_{el}^l + \epsilon_p^l \tag{2a}$$

$$\epsilon_a^d = \epsilon_{el}^d + \epsilon_p^d \tag{2b}$$

where

ϵ_{el}^l longitudinal elastic strain amplitude

ϵ_p^l longitudinal plastic strain

ϵ_{el}^d diametral elastic strain amplitude

ϵ_p^d diametral plastic strain

Also,

$$\epsilon_{el}^l = \frac{\Delta\epsilon_{el}^l}{2} = \frac{\sigma_a}{E} = \frac{\Delta\sigma}{2E} = \frac{\Delta P}{2AE} \tag{3a}$$

$$\epsilon_{el}^d = \frac{\Delta\epsilon_{el}^d}{2} = \mu\epsilon_{el}^l = \frac{\mu\,\Delta\sigma}{2E} = \frac{\mu\,\Delta P}{2AE} \tag{3b}$$

where E is the elastic modulus and μ is Poisson's ratio. The plastic term ϵ_p^l must be related to $\Delta\epsilon^d$ through the total plastic diametral strain ϵ_p^d. Figure 6 illustrates stresses and diametral strain components for a typical stress-strain hysteresis loop during fatigue. The width of this hysteresis loop is the measure of ϵ_p^d. The longitudinal plastic strain ϵ_p^l is equal in magnitude to twice ϵ_p^d (since volume is conserved during plastic flow) and is opposite in sign, alternating each cycle from tension to compression. Since comparison is desired with the tensile stress-strain curve, only positive strains need be considered. Hence,

$$\epsilon_p^l = 2\epsilon_p^d \tag{4a}$$

$$\epsilon_p^d = \Delta\epsilon^d - \Delta\epsilon_{el}^d = \Delta\epsilon^d - \frac{\mu\,\Delta P}{AE} \tag{4b}$$

$$\epsilon_p^l = 2\left(\Delta\epsilon^d - \frac{\mu\,\Delta P}{AE}\right) \tag{4c}$$

By substituting equations (3a) and (4c) into (2a), the desired relation is obtained:

$$\epsilon_a^l = \left(\frac{1}{2} - 2\mu\right)\frac{\Delta P}{AE} + 2\,\Delta\epsilon^d \tag{5}$$

The cyclic stress-strain relation was established for each material by plotting σ_a against ϵ_a^l as shown in figure 7. This curve defines the shakedown stress amplitude that accompanies a given strain limit during strain cycling loading. It is readily apparent, on comparison with the virgin tensile data, that very appreciable changes to the stress-strain relation are caused by cyclic straining. These figures also reveal cyclic strain-softening and strain-hardening behavior by the vertical displacement of the fatigue curve from the static tensile curve. Strain-softening materials exhibit a larger percentage reduction of stress at 1- or 2-percent strain (corresponding to intermediate life) than at 7- or 8-percent strain (corresponding to very short life). Apparently the softening characteristics are counteracted somewhat by large values of applied strain. On the other hand, strain-hardening materials tend to have a greater increase of stress at the larger strains.

Great differences exist between the stress-strain curves of initially annealed (or soft) and hardened conditions of an alloy. Figure 7 shows that strain-cycling fatigue causes the cyclic stress-strain relations for the two initial hardness conditions to become much more alike. This effect is most pronounced for materials that are customarily hardened by working such as AISI 304 and AM 350, though it does occur to a lesser degree with heat-treatable steels such as AISI 4130 and 4340.

Although the degree of softening or hardening varies somewhat with applied strain, an approximate comparison of materials with respect to these characteristics can be made by evaluating the ratio of the shakedown stress in fatigue at a given strain range to the virgin tensile stress at a corresponding value of strain. This ratio is less than unity for cyclic strain softening and greater than unity for cyclic strain hardening. Table IV lists this ratio, calculated at 1-percent strain, for each material (in order of increasing value). A fair correlation exists between the degree of softening or hardening and the parameter σ_u/σ_{ys} (ultimate tensile strength σ_u divided by the conventional 0.2-percent offset yield strength σ_{ys}, fig. 8). All materials for which $\sigma_u/\sigma_{ys} = 1.2$ or less softened under cyclic straining and those for which $\sigma_u/\sigma_{ys} = 1.4$ or greater strain hardened. At intermediate values, $1.2 < \sigma_u/\sigma_{ys} < 1.4$, both hardening and softening were observed. This correlation may serve as a guide for estimating from tensile test data the degree of hardening or softening that may be expected in the absence of the requisite fatigue data.

The practical use of cyclic stress-strain relations in conjunction with the strain-life relations, which will be discussed next, for the application to the solution of practical problems is demonstrated in reference 8.

Relation of Life to Total Strain and to Elastic and Plastic Components

For the most general of design applications, it is necessary to know the relation of fatigue life to both the total mechanical strain and the elastic and plastic components of this strain. Basic experimental strain-life test data are necessary also to evaluate and devise methods of predicting fatigue life and to obtain a better understanding of notch behavior in fatigue. These purposes are served by the experimental strain-life data shown for each test material in figure 9. Plotted on log-log coordinates are the elastic strain range $\Delta\epsilon_{el}^{l}$, plastic strain ϵ_p^l, and total strain range $\Delta\epsilon^l$ against N_f for each fatigue test. The elastic strain range and the plastic strain component are calculated from the basic data using equations (3a) and (4c), respectively. The total strain range $\Delta\epsilon^l$ equals the sum of these elastic and plastic components.

Some general observations can be made about the behavior of the various strain data. The plastic strain, for example, has a magnitude many times that of the elastic strain range at short life, but it decreases rapidly with increasing life to become negligible in comparison with $\Delta\epsilon_{el}^{l}$ at long life. This is true for all the test materials except in the long-life region for AISI 304 ELC annealed and AM 350 annealed (figs. 9(f) and (i)), where the plastic strain remains a significant quantity though less than the elastic component.[1] The relative tolerance of different materials to plastic strain in the short-life region seems

[1]The anomalous behavior of these strongly strain hardening stainless steels, as well as the delayed hardening of these steels at the low strain levels (figs.

to correlate quite directly with the tensile ductility. Those materials with larger ductilities such as 1100 aluminum and AISI 304 annealed withstand a greater plastic strain for a given life than those with low ductilities such as beryllium and Inconel X.

Figure 9 also indicates that a log-log representation of plastic strain against fatigue life for most materials can be fitted well with a straight line (again except for the annealed states of AISI 304 ELC and AM 350). In determining the least-squares straight-line fit shown in figure 9, all data were used except those for fatigue lives less than 10 cycles and those for which the plastic strain is less than one-half the elastic strain range. The former exclusion is made because, under these large load and plastic flow conditions, bending in the test section often takes place or the diametral strain-gage fixture often indents the test section or both. The strain and load readings for these very short lives, therefore, may be open to some question. The latter exclusion is made because any error of fixed magnitude that enters into the calculated plastic strain becomes an increasingly larger percentage of the strain as it decreases to low values. Therefore, for the purposes of subsequent detailed analysis (ref. 10) the line was fitted to the more representative data. It is obvious that empirical mathematical relations such as this straight-line correlation may work out very well in the short-life region where the plastic strain is large. However, for small values of plastic strain, on the order of 0.001 inch per inch or less, large errors in predicted life may result because of the uncertainty of the straight-line extrapolation into this region and because of uncertainties in E, μ, and other factors that enter into the ϵ_p calculation. Consequently, such a method, at best, would be limited to a maximum life of about 800 cycles for materials like AM 350 (hard) or 4000 cycles for those like AISI 52100.

The elastic strain range, unlike the plastic strain, never decreases to diminishingly small values that are impossible to measure or calculate accurately. Hence, it could be practical to relate fatigue life with the elastic strain (or stress) over the entire life span. This might be done in a way similar to that used for the plastic component, that is, by also fitting the elastic data with a single straight line. For many of the test materials such a correlation represents the data well over the range investigated, but for others there is a tendency for the data points to fall off such a line in either the long- or short-life region. The straight lines fitted to the elastic strain data of figure 9 represent the least-squares fit of all failure data except those cases in the short-life region where the elastic strain is less than one-half of the plastic strain. This straight-line method of representation again was chosen for purposes used in reference 10 in which equations representing the elastic and plastic components are summed up to develop a relation between total strain range and

4(f) and (i)), appears to be associated with the transformation of austenite to the body-centered lattice that takes place during cyclic strain fatigue (ref. 9). The transformation, which is evidenced by an increase in magnetic properties during the test, proceeds at a much slower rate at the lower strain levels than the high. It appears to go to completion at high strain levels (as evidenced by magnetic properties and stress range behavior) well before specimen failure, but only partial transformation is accomplished at failure under low strain levels.

cyclic life. Such relations provide the designers with complete information concerning stress, strain, and fatigue life.

Figures 9(a) to (p) also demonstrate the behavior of total longitudinal strain range with cyclic life for the test materials. In most cases $\Delta\epsilon^l$ decreases very rapidly with increasing N_f in the short-life region and then changes much less rapidly in the intermediate life region. This behavior of total strain reflects, of course, the overriding effect that the plastic strain component has upon total strain in the short-life region and the predominant effect the elastic strain component has in the longer life region. By adding together, at a given life, the strain values denoted by the straight-line correlation of the elastic and plastic strain components the corresponding correlating line for total strain can be determined. This line represents test data well for most of the materials, indicating that the total strain against life relations can be obtained by summing up the elastic and plastic components as approximated by straight-line relations. The biggest exceptions occur in the longer life region of the annealed states of AISI 304 and AM 350, which is apparently due to the previously mentioned transformation that takes place in these materials.

Relative Performance of Materials

Comparison on basis of diametral strain range. - Figure 10 illustrates the effect of diametral strain range $\Delta\epsilon^d$ on fatigue life for all the materials where this was the independent test variable. At a specific life the spread in $\Delta\epsilon^d$ is greatest in the short-life region, becomes small at about 10,000 cycles, and then becomes fairly large again in the long-life region. A close examination of the data reveals that the relative standings of materials change with N_f. For example, 1100 aluminum and AISI 4130 (soft) steel withstand the greatest $\Delta\epsilon^d$ for short lives, but they rate among the poorest at long life. Conversely, AM 350 (annealed) shows up poorly at short life, but it is one of the best for fatigue lives of 10^5 to 10^6 cycles. Table V, derived from this figure, makes a detailed comparison of the diametral strain range capability for the various materials at fatigue lives of 100, 3000, and 100,000 cycles. The strain range capability of the best material is about 6 times that of the poorest at 100 cycles, only $1\frac{1}{2}$ times greater at 3000 cycles, and 3 times greater at 100,000 cycles. The change in relative ratings in going from short to long life is plainly evident. Titanium (6Al-4V) is an exception to the general trend since it ranks as one of the better strain-resisting materials over the complete life range.

The fact that the relative strain-cycling performance of materials changes with N_f is due to their different tolerances to plastic strain and elastic strain (or stress). In the short-life region the materials with the greatest plastic strain absorbing capacity (most ductile) will show up best, and in the long-life region generally those with the greatest elastic strain absorbing capacity (best endurance limit) will excel. For moderate life, 1000 to 10,000 cycles, the better materials are those with the best combination of plastic plus elastic strain capacity.

Stress range comparison. - Stress range at $\frac{1}{2} N_f$ is plotted against $\log N_f$ in figure 11 for all test materials. There is less change in the relative ratings of the materials with increasing life than there is when comparison is made on a cyclic strain basis. Aluminum and beryllium fall well below the steels; however, on a strength-to-density basis these materials would be comparable to the steels, and titanium (6Al-4V) would rank highest. Table VI indicates the small variation of relative ratings of materials on a stress range basis for fatigue lives of 100, 3000, and 100,000 cycles. Comparison with table V shows stress range ratings of materials to be almost the inverse of the strain range at N_f = 100 cycles.

Notch sensitivity. - Under certain test conditions for some materials fatigue failure took place outside the test section in a region of stress concentration. Although it was not the purpose of this test program to investigate systematically the effect of stress concentrations, the previously discussed strain-life relations explain the observed behavior very well. These nontest-section fractures never occurred during very high strain range tests (corresponding to short lives) but, rather, appeared at some critical lower strain level and at all strain ranges less than this critical value. In other words, certain materials exhibited sensitivity to a particular type of stress raiser when subjected to applied strain ranges below, but not above, some critical value.

Materials showing this behavior were AISI 4130 (hard), AISI 52100, AM 350 (hard), and titanium (6Al-4V). Two of these, AISI 4130 (hard) and 52100, were tested in the threaded-head configuration (fig. 1(b)). Nontest-section failures occurred at the innermost thread root at one end of the specimen. The only other material tested with threaded ends, AISI 4130 (soft), did not show notch sensitivity. AM 350 (hard) and titanium, like most of the materials, were made into buttonhead specimens (fig. 1(a)). Nontest-section failures originated at the small fillet joining the buttonhead at the 1/2-inch-diameter shoulder. Once these failures were observed, it was necessary to reduce the test-section diameter to obtain strain-life data in the longer life region. Such a change is effective, of course, because it reduces the ratio of strain at the notch to that at the test section.

In order to use the strain-life relations to explain this behavior it is necessary to relate the localized total strain range at the stress raiser $\Delta\epsilon_{sr}^{l}$ to the uniform elastic strain range $\Delta\epsilon_{el}^{l}$ at the test section and then to compare $\Delta\epsilon_{sr}^{l}$ with $\Delta\epsilon^{l}$, the total strain range at the test section. Since both the test section and stress raiser are subject to the same load range ΔP, the nominal stress range at the stress raiser $\Delta\sigma_{sr}$ can be equated to the test-section stress range $\Delta\sigma$ as follows:

$$\Delta\sigma_{sr} = \frac{A}{A_{sr}} \Delta\sigma = m \Delta\sigma$$

where

A cross-sectional area at test section

A_{sr} cross-sectional area at stress raiser (thread root or shoulder)

m A/A_{sr}, a constant for a given specimen configuration

Localized total strain range at the stress raiser $\Delta\epsilon^{l}_{sr}$ is assumed to be approximately equal to the elastically computed strain range at this point multiplied by the elastic stress concentration factor k. This is a commonly used assumption that is sufficiently accurate for the present purpose. The total strain range at the stress raiser $\Delta\epsilon^{l}_{sr}$ can then be related to the elastic strain range at the test section $\Delta\epsilon^{l}_{el}$:

$$\Delta\epsilon^{l}_{sr} = k\,\frac{\Delta\sigma_{sr}}{E} = km\,\frac{\Delta\sigma}{E} = C\,\Delta\epsilon^{l}_{el}$$

where C is a constant equal to km.

If C is less than unity, the total strain range at the stress raiser is less than the elastic strain range at the test section and therefore must be less than the total strain range at the test section. Consequently, for $C < 1$, failure must occur at the test section. When C is greater than unity, the total strain range at the stress raiser is greater than the elastic strain range at the test section, and therefore may or may not be greater than the total strain range at the test section. Location of failure is dependent upon which of these total strain ranges is the larger. For this latter case consider figure 12, which presents elastic and total strain range as a function of life for AISI 52100 steel. A dotted line is drawn parallel to the elastic strain range line but is vertically displaced by the factor $C = 1.5$ to represent a hypothetical localized total strain at the thread root $\Delta\epsilon^{l}_{sr} = 1.5\,\Delta\epsilon^{l}_{el}$. This line intersects the test-section total strain range line at 700 cycles. For lives less than 700 cycles, $\Delta\epsilon^{l}$ is greater than $\Delta\epsilon^{l}_{sr}$; consequently, failure is expected at the test section. For lives greater than 700 cycles, $\Delta\epsilon^{l}_{sr}$ is greater than $\Delta\epsilon^{l}$, and fracture should take place at the notch. Qualitatively, this is the type of behavior that was observed in the abovementioned materials.

These strain-life relations can be used further to make comparisons of the relative notch sensitivities of all test materials. An effective way of doing this is to compare characteristic strain ratio curves in which the ratio of total strain range divided by elastic strain range at the test section $\Delta\epsilon^{l}/\Delta\epsilon^{l}_{el}$ (obtained from the strain-life test data) is plotted against $\log N_f$, as has been done in figure 13 for the three materials tested in the threaded-head configuration. Now, whenever the total strain at the stress raiser is less than that at the test section, failure should occur at the test section. In other words, if $\Delta\epsilon^{l}_{sr}/\Delta\epsilon^{l}_{el} = C$ is less than the characteristic strain ratio $\Delta\epsilon^{l}/\Delta\epsilon^{l}_{el}$, failure

takes place at the test section; if C is greater than the characteristic strain ratio, failure takes place at the stress raiser. As an example, consider again the hypothetical case where $C = 1.5$; that is, the total strain range at the stress raiser is $1\frac{1}{2}$ times the elastic strain range at the test section. The ordinate on the right side of the graph is used to represent $\Delta\epsilon^l_{sr}/\Delta\epsilon^l_{el} = C$, which, for a specific specimen geometry, is a fixed value independent of N_f. The dashed line at $C = 1.5$ intersects the strain ratio - life curve of AISI 52100 steel at about 700 cycles. If failure is to occur anywhere in the specimen at less than 700 cycles, it should take place in the test section because $\Delta\epsilon^l$ is greater than $\Delta\epsilon^l_{sr}$ in this life region. If failure occurs at more than 700 cycles, it should take place at the stress raiser since $\Delta\epsilon^l_{sr}$ exceeds $\Delta\epsilon^l$ in this region. This intercept occurs at about 7000 cycles for AISI 4130 (hard) and 17,000 cycles for AISI 4130 (soft). The value of life at which this transition from test-section to stress-raiser-type failure occurs is then a measure of fatigue notch sensitivity. Notch sensitivity decreases with increasing values of "transition" life.

These characteristic strain ratio curves indicate that AISI 52100 would be more notch sensitive than AISI 4130 (hard), which in turn is more notch sensitive than AISI 4130 (soft) regardless of C, since the curves do not cross one another. Tests results for the standard 0.25-inch-diameter test section substantiate this observation. The least number of cycles causing a thread failure was 225 for AISI 52100 steel and 15,500 for AISI 4130 (hard). No thread failures took place in AISI 4130 (soft) even for fatigue lives exceeding one million cycles. Similar characteristic strain ratio comparisons (fig. 14) for the materials tested in the buttonhead configuration indicate for $1 < C < 1.2$ that nontest-section failures should occur at the lowest life for AM 350 (hard) and next lowest life for titanium. Experiment indicated buttonhead failures in as few as 23,200 cycles for AM 350 (hard) and 192,000 cycles for titanium. No such failures developed in the other materials.

A more quantitative application of this analysis could not be accurately applied to these data for several reasons. First, the value of stress concentration factor k is not accurately known. Roark (ref. 11) quotes k for similar configurations; however, he does not give the values for geometries as severe as those used. Second, this method of analysis should be useful for the prediction of the initiation of a fatigue crack at the stress raiser, but not necessarily for the prediction of complete separation of the entire specimen cross section. Crack propagation may have an appreciable effect upon life, depending upon the duration of the macrostage of crack growth (ref. 12, pp. 22-25). The appearance of test-section fracture surfaces indicated that the size of the fatigued area was less for high-yield-strength materials than for low; also the fatigued area for a given material tended to be less at high strain levels than at low levels. The quantitative analysis can be particularly difficult when C is close to unity for these reasons and other reasons such as the uncertainty in the $\Delta\epsilon^l/\Delta\epsilon^l_{el}$ ratio and the material effect upon the k value.

CONCLUSIONS

The following conclusions are based upon extensive strain-cycling tests about a zero mean strain and apply to AISI 4130 (soft and hard conditions), AISI 4340 (annealed and hard), AISI 52100 (hard), AISI 304 ELC (annealed and hard), AISI 310 (annealed), AM 350 (annealed and hard), Inconel X, titanium (6Al-4V), 2014-T6, 5456-H311, and 1100 aluminum, and beryllium materials:

1. The cyclic stress-strain relations have been established and are shown to be substantially different from the virgin tensile data in many instances.

2. These relations are based upon the general observation that the stress range, following the initial period in which cyclic strain hardening or softening occurred, remains relatively unchanged throughout the majority of the specimen life.

3. A fair correlation was obtained between the degree of cyclic strain hardening and softening and the ratio of ultimate strength over yield strength. Hardening always took place when this ratio exceeded 1.4, and the softening occurred when the ratio was less than 1.2.

4. The life relation between elastic, plastic, and total strain components has been established. Straight-line fits of the logarithmic elastic strain-life and plastic strain-life data, when summed together, provide good agreement with the total strain range - life data for metallurgically stable materials.

5. The test data can be used to evaluate relative performance of all test materials both on a strain range and stress range basis over a life span of a few cycles up to one million cycles.

6. In general, the materials with the better total strain-absorbing capacity at low life (100 cycles or less) were among the poorest at high life (100,000 cycles or more). Titanium (6Al-4V), which had good performance throughout the entire life span, was an exception to this behavior.

7. The strain-life relations can be used to explain the changes in susceptibility to stress concentrations over a large life span and to rate correctly the relative notch sensitivities of the four test materials that experienced nontest-section failures in comparison with the other test materials.

Lewis Research Center
National Aeronautics and Space Administration
Cleveland, Ohio, October 10, 1962

APPENDIX A

SYMBOLS

A	cross-sectional area of test section, sq in.
C	dimensionless constant
E	modulus of elasticity, lb/sq in.
k	stress concentration factor
m	area ratio
N	number of cycles
N_f	number of cycles to failure
ΔP	load range, lb
ϵ	strain, in./in.
$\Delta\epsilon$	strain range, in./in.
μ	Poisson's ratio
σ	stress, lb/sq in.
$\Delta\sigma$	stress range, lb/sq in.

Subscripts:

a	amplitude
el	elastic component of total strain
f	fracture
max	maximum value during a fatigue cycle
min	minimum value during a fatigue cycle
p	plastic component of total strain
sr	at stress raiser
u	ultimate
ys	0.2-percent offset yield strength

Superscripts:

d diametral

l longitudinal

APPENDIX B

PRECAUTIONS TAKEN DURING BERYLLIUM TESTING

Since beryllium particles ingested into the body or deposited into open wounds are known to be toxic, special precautions were taken during beryllium testing to prevent dispersion of such dust particles into the test-room atmosphere. One likely source of beryllium dust in addition to that caused by test-section failure is due to fretting that can take place between the specimen alinement shoulders and the split-cone grips. To minimize the chances of developing airborne particles from these sources, the specimen was thoroughly coated with Lubriplate grease. Figure 15 illustrates the enclosure built around the specimen assembly and used to further prevent beryllium dust particles from entering the atmosphere. The enclosure was made of a longitudinally split plastic cylinder, 8 inches in outside diameter by 13 inches long by 1/4 inch thick, sealed at both ends with 1/16-inch-thick sheet rubber. Two diametrically opposite $1\frac{1}{2}$-inch-diameter holes in the plastic were provided for the passage of intake air into the chamber and for straight-through sighting of the Tuckerman gage with the autocollimator. Another $1\frac{1}{2}$-inch-diameter hole near the base of the cylinder served as an air exhaust port by the attachment of a vacuum cleaner hose. Exhaust air was filtered with Hollinsworth and Boss number 70 filter paper. The vacuum cleaner was operated continuously throughout the test and during disassembly of the fractured specimen at an approximate flow rate of 0.05 cubic meter per minute. Test operators wore protective clothing while assembling the setup, taking strain-gage readings, disassembling the apparatus, and washing down test specimen, grips, plastic cylinders, rubber seals, and so forth, after the test. A respirator was worn together with rubber gloves and a laboratory coat.

In order to obtain data that might be used to evaluate the degree of hazard involved, emission spectrographic analyses of air filter and smear swabs taken from various parts of the apparatus were made following a fatigue test of about $1\frac{1}{2}$-hour duration (1376 cycles). Whatman number 41H filter paper disks about $2\frac{3}{16}$ inch in diameter were used for the swabs. Results of the analysis made by a commercial spectrographic company, which reported a sensitivity of 0.01 microgram of beryllium, are the following:

Sample source	Be content, micrograms/sample
Air filter	<0.1
Test specimen (fractured portion and shoulders)	15.00
Rubber pad beneath cylinder	3.5
Inside surfaces of plastic cylinder	.30
Lubriplate as it comes from supply can	.15

The amount of beryllium trapped out from the exhausted air is low, and, with further substantiating data, might indicate that the respirator and specimen enclosure is not necessary. The greater amounts of apparently larger beryllium particles found on the greased specimen and the rubber pad suggest that a careful cleanup after each test is desirable.

REFERENCES

1. Manson, S. S.: Behavior of Materials Under Conditions of Thermal Stress. NACA Rep. 1170, 1954. (Supersedes NACA TN 2933, 1953.)

2. Coffin, L. F., Jr.: A Study of the Effects of Cyclic Thermal Stresses on a Ductile Metal. Trans. ASME, vol. 76, no. 6, Aug. 1954, pp. 931-949; discussion, pp. 949-950.

3. Coffin, L. F., Jr.: Design Aspects of High Temperature Fatigue with Particular Reference to Thermal Stresses. Trans. ASME, vol. 78, no. 3, Apr. 1956, pp. 527-532.

4. Kooistra, L. F.: Effect of Plastic Fatigue on Pressure Vessel Materials and Design. Welding Jour. (Welding Res. Supplement), vol. 36, Mar. 1957, pp. 120S-130S.

5. Manson, S. S.: Thermal Stresses in Design. Pt. 19 - Cyclic Life of Ductile Materials. Machine Design, vol. 32, no. 14, July 7, 1960, pp. 139-144.

6. Manson, S. S.: Thermal Stresses in Design. Pt. 20 - Thermal Cycling with Steady Stress. Machine Design, vol. 32, no. 15, July 21, 1960, pp. 161-167.

7. Langer, B. F.: Design of Pressure Vessels for Low-Cycle Fatigue. Paper 61-WA-18, ASME, 1961.

8. Manson, S. S.: Thermal Stresses in Design. Pt. 18. Working Stresses for Ductile Materials. Machine Design, vol. 32, no. 13, June 23, 1960, pp. 153-159. (See also pt. 19, vol. 32, no. 14, July 7, 1960, pp. 139-144.)

9. Brick, R. M., and Phillips, Arthur: Structure and Properties of Alloys. McGraw-Hill Book Co., Inc., 1942, p. 160.

10. Tavernelli, J. F., and Coffin, L. F., Jr.: Experimental Support for Generalized Equation Predicting Low-Cycle Fatigue (Discussion by S. S. Manson). Jour. Basic Eng. (Trans. ASME), ser. D, vol. 84, no. 4, Dec. 1962, pp. 537-541.

11. Roark, Raymond Jefferson: Formulas for Stress and Strain. Third ed., McGraw-Hill Book Co., Inc., 1954, pp. 348; 353.

12. Smith, Robert W., and Smith, Gordon T.: Thermal-Fatigue Crack-Growth Characteristics and Mechanical Strain Cycling Behavior of A-286, Discaloy, and 16-25-6 Austenitic Steels. NASA TN D-479, 1960.

TABLE I. - MATERIAL DESCRIPTION

Material	Nominal composition, percent	Condition	Hardness, Rockwell -
AISI 4130 (soft)	C 0.30, Mn 0.50, P 0.040, S 0.040, Si 0.28, Cr 0.95, Mo 0.20, Fe remainder	1700° F; 1/2 hr in salt, water quench 1200° F; 1/2 hr in salt, air cool	C-25 to 27
AISI 4130 (hard)	Same heat as above	1600° F; 1/2 hr in salt, water quench 750° F; 1 hr in salt, air cool	C-39 to 40
AISI 4340 (annealed)	C 0.40, Mn 0.70, P 0.040, S 0.040, Si 0.28, Ni 1.82, Cr 0.80, Mo 0.25, Fe remainder	Hot rolled and annealed by supplier	C-22 to 24
AISI 4340 (hard)	Same heat as above	1520° F; 1/2 hr in salt, water quench 800° F; 2 hr in salt, air cool	C-44
AISI 52100	C 1.02, Mn 0.35, P 0.025, S 0.025, Si 0.28, Cr 1.45, Fe remainder	1650° F; 1 hr in salt, air cool to room temp. 1535° F; 1 hr in salt, oil quench to 180° F Immediately temper 320° F, 35-min total time, air cool 775° F; 1-hr total time in salt, air cool	C-52 to 53
AISI 304 ELC (annealed)	[a]C 0.026, Mn 0.45, P 0.03, S 0.014, Si 0.40, Cr 18.67, Ni 8.50, Mo 0.02, Cu 0.10, Fe remainder	Hot rolled and annealed by supplier	B-82 to 84
AISI 304 ELC (hard)	Same heat as above	Cold drawn by supplier	C-34 to 36
AISI 310 (annealed)	C 0.25 max., Mn 2.00 max., Si 1.50 max., Cr 25.0, Ni 20.5, Fe remainder	Hot rolled, pickled, and annealed by supplier	B-75 to 81
AM 350 (annealed)	C 0.10, Mn 0.75, Si 0.35, Cr 16.50, Ni 4.25, Mo 2.75, N 0.10, Fe remainder	Hot rolled, pickled, and annealed by supplier	
AM 350 (hard)	Same heat as above	Cold drawn 25-35% reduction by supplier	C-50 to 52
Inconel X	C 0.04, Mn 0.70, Si 0.30, Cr 15, Cb 1, Ti 2.5, Al 0.9, Fe 7, Ni remainder	2100° F; 4 hr, air cool 1550° F; 24 hr, air cool 1300° F; 20 hr, air cool	C-34 to 35
Titanium (6Al-4V)	C 0.029, Fe 0.22, N_2 0.017, Al 6.1, V 4.0, H_2 0.007, Ti remainder	Centerless ground, solution treated, and aged by supplier	C-40 to 41
2014-T6 aluminum	Si 0.85, Fe 1.0, Cu 4.5, Mn 0.80, Mg 0.50, Cr 0.10 max., Zn 0.25 max., Ti 0.15 max., Al remainder	Bar stock as received	B-81 to 84
5456-H311 aluminum	Si + Fe 0.40 max., Cu 0.10 max., Mn 0.75, Mg 5.1, Cr 0.12, Zn 0.25, Ti 0.20, Al remainder	Bar stock as received	B-56
1100 aluminum	Si + Fe 1.0, Cu 0.20 max., Mn 0.05 max., Zn 0.10, Al remainder	Bar stock as received	BHN ~26
Beryllium	C 0.15 max., Mg 0.08 max., Si 0.12 max., Al 0.16 max., Fe 0.18 max., BeO 2.0 max., Be 98.0 min., other metal 0.04 max.	Vacuum hot-pressed QMV beryllium	B-75 to 90

[a]Actual analysis.

TABLE II. - MECHANICAL AND ELASTIC

PROPERTIES OF TEST MATERIALS

[Data represent the average of three test specimens unless otherwise specified.]

Material	Yield strength 0.2-percent offset strength, σ_{ys}, ksi	Ultimate strength, σ_u, ksi	Fracture strength, σ_f, ksi	Reduction in area, percent	True ductility	Modulus of elasticity, E	Poisson's ratio, μ
4130 (soft)	113	130	245	67.3	1.12	32×10^{-6}	0.29
4130 (hard)	197	207	302	54.7	.79	29	.28
4340 (ann.)	92	120	174	43.4	.57	28	.32
4340 (hard)	199	213	278	38.1	.48	29	.30
52100	279	292	323	11.2	.12	30	.29
304 ELC (ann.)	37	108	278	74.3	1.37	27	.27
304 ELC (hard)	108	138	295	68.8	1.16	25	.34
310 (ann.)	32	93	197	63.5	1.01	28	.30
350 (ann.)	64	191	339	52.1	.74	28	.32
350 (hard)	270	276	328	20.3	[a].23	26	.30
Inconel X	102	176	219	19.7	.22	31	.31
Titanium	172	179	249	41.0	.53	17	.33
2014-T6 Al	67	74	91	25.0	.29	10	.33
5456-H311 Al	34	58	82	34.6	.42	10	.33
1100 Al	14	16	(b)	87.6	2.09	[c]10	[c].33
Beryllium	38	46.9	47.7	1.7	.017	42	[d].024

[a]Data for five specimens ranged from 0.08 to 0.38.

[b]Could not be accurately measured.

[c]Assumed equal to value obtained for other aluminum alloys.

[d]Beryllium datum from commercial supplier.

TABLE III. - SUMMARY OF TEST DATA AND STRAIN CALCULATIONS FOR EACH TEST SPECIMEN

Stress range, $\Delta\sigma = \frac{P_{max} - P_{min}}{A}$, ksi	Fatigue life, N_f, cycles	Diametral elastic strain range, $\Delta\epsilon^d_{el}$, in./in.	Diametral plastic strain, ϵ^d_p, in./in.	Diametral total strain range, $\Delta\epsilon^d$, in./in. (a)	Longitudinal elastic strain range, $\Delta\epsilon^l_{el}$, in./in.	Longitudinal plastic strain, ϵ^l_p, in./in.	Longitudinal total strain range, $\Delta\epsilon^l$, in./in.	Comments
				AISI 4130 (soft)				
300	12	0.0025	0.1282	0.1260	0.0036	0.2504	0.2600	(b)
250	17	.0027	.0773	.0800	.0033	.1546	.1638	(c)
253	27	.0027	.0773	.0800	.0032	.1547	.1638	(b)
214	63	.0025	.0475	.0480	.0028	.0910	.0996	(b)
234	134	.0022	.0270	.0272	.0074	.0301	.0375	(d)
221	168	.0020	.0220	.0240	.0069	.0440	.0509	
210	248	.0019	.0191	.0210	.0067	.0381	.0448	
214	488	.0019	.0128	.0147	.0067	.0255	.0322	
150	672	.0017	.0038	.0113	.0059	.0192	.0251	
150	1,000	.0017	.0063	.0100	.0058	.0166	.0224	
170	1,580	.0016	.0056	.0066	.0058	.0100	.0158	
174	5,830	.0016	.0022	.0038	.0054	.0044	.0098	
200	7,260	.0015	.0023	.0038	.0053	.0043	.0096	
150	24,400	.0014	.0008	.0022	.0048	.0016	.0064	
150	32,300	.0014	.0008	.0022	.0048	.0012	.0060	
140	42,000	.0013	.0001	.0014	.0045	.0002	.0047	
150	96,400	.0014	0	.0013	.0047	0	.0047	
130	326,000	.0012	0	.0012	.0041	0	.0041	(e),(f)
14[illegible]	328,000	.0013	0	.0013	.0045	0	.0045	(e)
110	11,200,000	.0010	0	.0010	.0034	0	.0034	(e),(g)
120	12,000,000	.0011	0	.0011	.0037	0	.0037	(e),(g)
				AISI 4130 (hard)				
437	4	0.0042	0.1958	0.2000	0.0151	0.3916	0.4066	(b)
403	16	.0039	.0761	.0800	.0139	.1522	.1661	(b)
330	49	.0032	.0448	.0480	.0116	.0805	.1011	
303	86	.0029	.0211	.0240	.0104	.0421	.0526	
261	356	.0025	.0075	.0100	.0090	.0150	.0240	
282	360	.0027	.0120	.0147	.0097	.0240	.0337	
244	1,320	.0024	.0042	.0066	.0084	.0085	.0169	
228	7,590	.0022	.0016	.0038	.0076	.0032	.0110	
223	18,500	.0022	.0006	.0028	.0079	.0012	.0091	(h),(i)
200	27,700	.0020	0	.0020	.0071	0	.0071	(h)
222	23,900	.0021	0	.0020	.0077	0	.0077	(j)
200	37,110	.0019	0	.0018	.0069	0	.0069	(j)
140	844,000	.0014	0	.0013	.0050	0	.0050	(j),(g)
150	2,030,000	.0015	0	.0015	.0054	0	.0054	(j),(g)
				AISI 4340 (annealed)				
292	7	0.0033	0.1167	0.1200	0.0104	0.2333	0.2438	(k)
272	14	.0031	.0769	.0800	.0097	.1538	.1635	(k)
232	43	.0027	.0373	.0400	.0083	.0747	.0830	(c)
192	168	.0022	.0178	.0200	.0069	.0356	.0425	
171	635	.0020	.0120	.0140	.0061	.0241	.0302	
153	1,050	.0018	.0082	.0100	.0057	.0164	.0220	
143	2,730	.0016	.0040	.0056	.0051	.0079	.0130	
124	14,000	.0014	.0018	.0032	.0044	.0036	.0080	(f)
114	81,200	.0013	.0007	.0020	.0041	.0014	.0055	
103	166,000	.0012	.0004	.0016	.0039	.0007	.0046	
104	824,000	.0012	.0002	.0014	.0037	.0004	.0041	
				AISI 4340 (hard)				
470	2	0.0049	0.1951	0.2000	0.0162	0.3903	0.4065	(b)
424	4	.0044	.1956	.2000	.0146	.3912	.4058	(c)
390	13	.0041	.0759	.0800	.0137	.1519	.1656	(c),(l)
398	51	.0041	.0359	.0400	.0137	.0718	.0855	(b)
378	52	.0039	.0361	.0400	.0130	.0722	.0852	(b)
333	192	.0034	.0166	.0200	.0115	.0331	.0446	
296	986	.0031	.0069	.0100	.0102	.0139	.0241	
254	2,850	.0026	.0036	.0062	.0088	.0059	.0147	
236	9,810	.0025	.0007	.0032	.0082	.0015	.0097	
230	30,700	.0024	0	.0020	.0079	0	.0079	
203	63,100	.0021	0	.0020	.0070	0	.0070	
17[illegible]	162,000	.0018	0	.0017	.0060	0	.0060	
17[illegible]	176,000	.0018	0	.0018	.0060	0	.0060	
160	3[illegible]4,200	.0016	0	.0014	.0052	0	.0052	(g)

TABLE III. - CONTINUED. SUMMARY OF TEST DATA AND STRAIN CALCULATIONS FOR EACH TEST SPECIMEN

Stress range at $\frac{1}{2} N_f$, $\Delta\sigma$, ksi	Fatigue life, N_f, cycles	Diametral elastic strain range, $\Delta\epsilon^d_{el}$, in./in.	Diametral plastic strain, ϵ^d_p, in./in.	Diametral total strain range, $\Delta\epsilon^d$, in./in. (a)	Longitudinal elastic strain range, $\Delta\epsilon^l_{el}$, in./in.	Longitudinal plastic strain, ϵ^l_p, in./in.	Longitudinal total strain range, $\Delta\epsilon^l$, in./in.	Comments
				AISI 52100				
621	2	0.0060	0.0420	0.0480	0.0207	0.0840	0.1047	
608	3	.0059	.0501	.0560	.0203	.1002	.1205	
610	4	.0059	.0341	.0400	.0203	.0682	.0885	(b)
602	5	.0058	.0302	.0360	.0202	.0603	.0805	(b)
579	10	.0056	.0344	.0400	.0193	.0688	.0881	
571	15	.0055	.0225	.0280	.0190	.0450	.0640	(b)
560	18	.0054	.0266	.0320	.0197	.0532	.0718	
553	18	.0053	.0187	.0240	.0184	.0373	.0557	(b)
514	40	.0050	.0150	.0200	.0171	.0301	.0472	
520	44	.0050	.0150	.0200	.0173	.0299	.0473	
483	73	.0047	.0113	.0160	.0161	.0227	.0388	
456	98	.0044	.0076	.0120	.0152	.0152	.0304	
468	159	.0045	.0083	.0128	.0156	.0166	.0322	
---	225	----	.0080	.0080	----	.0160	.0160	(h)
386	728	.0037	.0031	.0068	.0129	.0061	.0190	
374	1,110	.0036	.0016	.0052	.0125	.0032	.0156	(i)
---	1,470	----	.0040	.0040	----	.0080	.0080	(h)
350	3,430	.0034	.0006	.0040	.0117	.0012	.0129	(i)
---	5,640	----	.0024	.0024	----	.0048	.0048	(h)
331	7,840	.0032	0	.0030	.0110	0	.0110	(i)
---	9,910	----	.0026	.0026	----	.0052	.0052	(h)
273	30,200	.0026	0	.0024	.0091	0	.0091	(i)
182	391,000	.0018	0	.0017	.0061	0	.0061	(j),(a)
217	799,000	.0021	0	.0020	.0072	0	.0072	(j)
				AISI 304 ELC (annealed)				
343	25	0.0034	0.0446	0.0480	0.0127	0.0891	0.1018	(b),(f)
315	55	.0031	.0288	.0320	.0117	.0577	.0694	(b),(f)
329	110	.0033	.0167	.0200	.0122	.0334	.0456	(b)
274	210	.0027	.0101	.0128	.0101	.0201	.0303	
280	396	.0025	.0039	.0064	.0093	.0078	.0171	
209	1,970	.0021	.0019	.0040	.0077	.0038	.0116	
174	6,010	.0017	.0015	.0032	.0064	.0029	.0094	
162	9,460	.0016	.0016	.0032	.0060	.0032	.0092	
110	40,400	.0011	.0013	.0024	.0041	.0026	.0067	
114	46,300	.0011	.0013	.0024	.0042	.0025	.0067	
103	143,000	.0010	.0010	.0020	.0038	.0019	.0056	
100	174,000	.0010	.0011	.0021	.0037	.0022	.0059	
90	832,000	.0009	.0009	.0018	.0033	.0018	.0051	
				AISI 304 (hard)				
350	31	0.0048	0.0452	0.0500	0.0140	0.0905	0.1045	(b),(c)
343	46	.0047	.0353	.0400	.0137	.0707	.0844	(b),(c)
311	138	.0042	.0158	.0200	.0124	.0316	.0440	(b)
314	208	.0043	.0117	.0160	.0126	.0235	.0360	(b)
274	1,320	.0037	.0035	.0072	.0110	.0069	.0179	
262	1,660	.0036	.0028	.0064	.0105	.0057	.0162	
206	7,780	.0028	.0008	.0036	.0082	.0016	.0098	
197	27,500	.0025	.0005	.0030	.0075	.0009	.0084	
150	95,000	.0020	.0004	.0024	.0060	.0007	.0067	
135	121,000	.0018	.0002	.0020	.0054	.0003	.0057	
125	474,000	.0017	.0001	.0018	.0050	.0002	.0052	
				AISI 310 (annealed)				
284	12	0.0030	0.1170	0.1200	0.0101	0.2339	0.2441	(b),(c)
282	23	.0030	.0770	.0800	.0101	.1540	.1640	(b),(c)
260	32	.0028	.0572	.0600	.0093	.1144	.1237	(b)
216	91	.0023	.0277	.0300	.0078	.0553	.0631	(c)
222	95	.0024	.0276	.0300	.0079	.0552	.0632	(i)
163	335	.0017	.0123	.0140	.0058	.0245	.0303	
134	1,400	.0014	.0066	.0080	.0048	.0131	.0179	
107	5,120	.0011	.0033	.0044	.0038	.0065	.0103	
83	30,000	.0009	.0011	.0020	.0030	.0022	.0052	(g)
79	55,200	.0008	.0010	.0018	.0028	.0019	.0047	
75	61,000	.0008	.0008	.0016	.0027	.0016	.0043	
70	173,000	.0008	.0006	.0012	.0025	.0009	.0034	
68	223,000	.0007	.0005	.0012	.0023	.0010	.0033	(g)
63	274,000	.0007	.0003	.0010	.0022	.0007	.0029	(i)
64	363,000	.0007	.0002	.0009	.0023	.0005	.0027	

TABLE III. - CONTINUED. SUMMARY OF TEST DATA AND STRAIN CALCULATIONS FOR EACH TEST SPECIMEN

Stress range at $\frac{1}{2}$ N_f, $\Delta\sigma$, ksi	Fatigue life, N_f, cycles	Diametral elastic strain range, $\Delta\epsilon^d_{el}$, in./in.	Diametral plastic strain, ϵ^d_p, in./in.	Diametral total strain range, $\Delta\epsilon^d$, in./in. (a)	Longitudinal elastic strain range, $\Delta\epsilon^l_{el}$, in./in.	Longitudinal plastic strain, ϵ^l_p, in./in.	Longitudinal total strain range, $\Delta\epsilon^l$, in./in.	Comments
				AM 350 (annealed)				
499	7	0.0057	0.0343	0.0400	0.0178	0.0686	0.0864	(b),(c)
501	18	.0057	.0183	.0240	.0179	.0365	.0544	(b),(c)
462	34	.0053	.0087	.0140	.0165	.0174	.0339	
422	125	.0048	.0032	.0080	.0151	.0064	.0214	
367	228	.0042	.0018	.0060	.0131	.0036	.0167	
288	1,134	.0033	.0015	.0048	.0103	.0030	.0133	
234	3,220	.0027	.0013	.0040	.0084	.0027	.0110	
193	15,410	.0022	.0012	.0034	.0069	.0024	.0093	
141	42,700	.0016	.0010	.0026	.0050	.0020	.0070	
152	98,300	.0017	.0011	.0028	.0054	.0021	.0076	
159	137,000	.0018	.0012	.0030	.0057	.0024	.0080	
134	170,000	.0015	.0011	.0026	.0048	.0021	.0069	
117	1,020,000	.0013	.0007	.0020	.0042	.0013	.0055	(g)
				AM 350 (hard)				
579	3	0.0067	0.0453	0.0520	0.0223	0.0906	0.1129	
567	14	.0065	.0235	.0300	.0218	.0469	.0687	
536	46	.0062	.0178	.0240	.0206	.0356	.0562	
525	71	.0061	.0139	.0200	.0202	.0279	.0481	
523	85	.0060	.0080	.0140	.0201	.0159	.0360	
524	90	.0060	.0140	.0200	.0202	.0279	.0481	
488	169	.0056	.0024	.0080	.0188	.0047	.0235	
522	176	.0060	.0080	.0140	.0201	.0160	.0360	
466	190	.0054	.0014	.0068	.0179	.0028	.0208	
436	450	.0050	.0010	.0060	.0168	.0019	.0187	
316	5,971	.0036	.0004	.0040	.0122	.0007	.0129	
272	11,500	.0031	.0001	.0032	.0105	.0001	.0106	
237	13,920	.0027	0	.0028	.0091	.0001	.0092	(j)
225	16,300	.0026	0	.0025	.0087	0	.0087	(j)
241	23,200	.0028	0	.0028	.0093	0	.0093	(h)
213	35,940	.0025	0	.0024	.0082	0	.0082	(h)
234	40,050	.0027	.0001	.0028	.0090	.0002	.0092	(j),(m)
220	56,600	.0025	0	.0025	.0085	0	.0085	(j),(m)
223	133,000	.0026	0	.0026	.0086	.0001	.0087	(j),(m)
219	759,000	.0025	0	.0025	.0084	0	.0084	(j),(m),(g)
227	1,010,000	.0026	0	.0026	.0087	0	.0087	(j),(m),(e)
				Inconel X				
382	2	0.0038	0.0682	0.0720	0.0123	0.1364	0.1487	(k)
422	4	.0042	.0518	.0560	.0136	.1036	.1172	(k)
396	6	.0040	.0400	.0440	.0128	.0801	.0929	(b)
408	9	.0041	.0379	.0420	.0132	.0758	.0890	(k)
378	37	.0038	.0322	.0360	.0122	.0644	.0766	(b)
368	41	.0037	.0303	.0340	.0119	.0606	.0725	(b)
356	50	.0036	.0304	.0340	.0115	.0609	.0724	(c)
336	79	.0034	.0268	.0300	.0108	.0533	.0641	
359	69	.0036	.0244	.0280	.0116	.0488	.0604	(b)
342	137	.0034	.0206	.0240	.0110	.0412	.0522	(b)
322	193	.0032	.0148	.0180	.0104	.0296	.0399	(i)
312	220	.0031	.0129	.0160	.0101	.0258	.0358	
314	261	.0031	.0169	.0200	.0101	.0337	.0438	
317	282	.0032	.0128	.0160	.0102	.0257	.0359	
298	296	.0030	.0070	.0100	.0096	.0140	.0237	
288	779	.0029	.0071	.0100	.0093	.0142	.0235	
281	813	.0028	.0072	.0100	.0091	.0144	.0234	
281	1,080	.0028	.0040	.0068	.0091	.0080	.0170	
264	1,580	.0026	.0024	.0050	.0085	.0047	.0132	
233	5,160	.0023	.0011	.0034	.0075	.0021	.0097	
232	5,210	.0023	.0017	.0040	.0075	.0034	.0108	
230	6,440	.0023	.0005	.0028	.0074	.0010	.0084	
231	7,800	.0023	.0005	.0028	.0075	.0010	.0084	
211	9,400	.0021	.0001	.0022	.0068	.0002	.0070	
215	9,940	.0021	.0008	.0029	.0069	.0015	.0085	
204	18,400	.0020	0	.0019	.0066	0	.0066	
188	36,400	.0019	0	.0018	.0061	0	.0061	
169	47,500	.0017	0	.0018	.0055	0	.0055	
155	99,800	.0015	0	.0014	.0050	0	.0050	
137	125,000	.0014	0	.0012	.0044	0	.0044	
124	267,000	.0012	0	.0012	.0040	0	.0040	
124	395,000	.0012	0	.0011	.0040	0	.0040	
114	688,000	.0011	0	.0010	.0037	0	.0037	

TABLE III. - CONTINUED. SUMMARY OF TEST DATA AND STRAIN CALCULATIONS FOR EACH TEST SPECIMEN

Stress range at $\frac{1}{2} N_f$, $\Delta\sigma$, ksi	Fatigue life, N_f, cycles	Diametral elastic strain range, $\Delta\epsilon^d_{el}$, in./in.	Diametral plastic strain, ϵ^d_p, in./in.	Diametral total strain range, $\Delta\epsilon^d$, in./in. (a)	Longitudinal elastic strain range, $\Delta\epsilon^l_{el}$, in./in.	Longitudinal plastic strain, ϵ^l_p, in./in.	Longitudinal total strain range, $\Delta\epsilon^l$, in./in.	Comments
Titanium (6Al-4V)								
430	6	0.0083	0.1117	0.1200	0.0253	0.2233	0.2486	(b)
382	27	.0074	.0646	.0720	.0225	.1292	.1516	(b)
338	86	.0066	.0294	.0360	.0199	.0589	.0788	
326	188	.0063	.0177	.0240	.0192	.0353	.0545	
313	453	.0061	.0079	.0140	.0184	.0158	.0343	
281	1,470	.0055	.0025	.0080	.0165	.0051	.0216	
216	11,800	.0042	0	.0040	.0127	0	.0127	
175	37,000	.0034	0	.0032	.0103	0	.0103	
156	70,200	.0030	0	.0028	.0092	0	.0092	
149	192,000	.0029	0	.0026	.0088	0	.0088	(h)
134	881,000	.0026	0	.0024	.0079	0	.0079	(h)
150	4,270,000	.0029	0	.0029	.0088	0	.0088	(j),(m),(e),(g)
172	5,590,000	.0033	0	.0033	.0101	0	.0101	(j),(m),(e),(g)
2014-T6 aluminum								
166	4	0.0055	0.0825	0.0880	0.0166	0.1650	0.1816	
147	10	.0048	.0552	.0600	.0146	.1103	.1250	
155	42	.0051	.0249	.0300	.0155	.0498	.0653	
142	203	.0047	.0093	.0140	.0142	.0186	.0328	
127	608	.0042	.0038	.0080	.0127	.0076	.0203	
117	1,610	.0039	.0009	.0048	.0117	.0019	.0136	
117	1,980	.0039	.0009	.0048	.0117	.0019	.0136	
107	4,180	.0035	.0001	.0036	.0106	.0002	.0108	
72	61,700	.0024	0	.0022	.0071	0	.0071	
92	95,550	.0030	0	.0029	.0091	0	.0091	
62	229,000	.0020	0		.0062	0	.0062	
67	285,000	.0022	0	.0020	.0066	0	.0066	
58	394,000	.0019	0	.0018	.0058	0	.0058	(g)
58	418,000	.0019	0		.0058	0	.0058	
5456-H311 aluminum								
138	7	0.0046	0.0554	0.0600	0.0138	0.1109	0.1247	(c)
133	12	.0044	.0476	.0520	.0133	.0952	.1085	
127	54	.0042	.0258	.0300	.0127	.0516	.0643	
118	175	.0039	.0101	.0140	.0118	.0202	.0320	
111	494	.0036	.0044	.0080	.0110	.0087	.0198	
100	1,920	.0033	.0015	.0048	.0100	.0030	.0130	
88	5,950	.0029	0	.0028	.0087	0	.0087	
72	22,800	.0024	0	.0022	.0072	0	.0072	
65	65,100	.0021	0	.0020	.0065	0	.0065	
59	90,300	.0019	0	.0018	.0059	0	.0059	
52	130,000	.0017	0	.0016	.0052	0	.0052	
47	366,000	.0015	0	.0014	.0047	0	.0047	
44	917,000	.0015	0	.0014	.0044	0	.0044	
1100 aluminum								
37	2	0.0012	0.2388	0.2400	0.0037	0.4776	0.4813	
37	2	.0012	.2388	.2400	.0037	.4776	.4812	
42	5	.0014	.2186	.2200	.0042	.4372	.4414	
42	11	.0014	.1986	.2000	.0042	.3972	.4014	
36	27	.0012	.1188	.1200	.0036	.2376	.2412	
30	73	.0010	.0590	.0600	.0030	.1180	.1210	
24	282	.0008	.0292	.0300	.0024	.0584	.0608	
22	784	.0007	.0133	.0140	.0021	.0266	.0287	
18	2,120	.0006	.0054	.0060	.0018	.0108	.0126	
18	6,320	.0006	.0024	.0030	.0018	.0048	.0066	
17	12,800	.0006	.0014	.0020	.0017	.0029	.0046	
15	104,000	.0005	.0005	.0010	.0015	.0010	.0025	
15	205,000	.0005	.0003	.0008	.0015	.0006	.0021	
15	417,000	.0005	.0002	.0006	.0015	.0003	.0018	
14	1,000,000	.0005	0	.0005	.0014	.0001	.0014	(g)

TABLE III. - CONCLUDED. SUMMARY OF TEST DATA AND STRAIN CALCULATIONS FOR EACH TEST SPECIMEN

Stress range at $\frac{1}{2} N_f$, $\Delta\sigma$, ksi	Fatigue life, N_f, cycles	Diametral elastic strain range, $\Delta\epsilon^d_{el}$, in./in.	Diametral plastic strain, ϵ^d_p, in./in.	Diametral total strain range, $\Delta\epsilon^d$, in./in. (a)	Longitudinal elastic strain range, $\Delta\epsilon^l_{el}$, in./in.	Longitudinal plastic strain, ϵ^l_p, in./in.	Longitudinal total strain range, $\Delta\epsilon^l$, in./in.	Comments
Beryllium								
117	6	0.0001	0.0066	0.0067	0.0028	0.0132	0.0160	
103	73	.0001	.0028	.0028	.0025	.0055	.0080	
82	138	0	.0010	.0011	.0020	.0020	.0040	
79	260	0	.0008	.0008	.0019	.0015	.0034	
66	4,260	0	.0004	.0005	.0016	.0008	.0024	

[a]Small discrepancies which appear upon comparison of the summation of elastic and plastic strain components with total strain arise because of small inaccuracies of the measured quantities E and μ. These cause errors in the fourth decimal place and sometimes result in the calculation of small negative plastic strains. In the table all negative plastic strains are reported as zero, but no change was made to the other calculated strains.

[b]Hourglass radius, 1 in.

[c]Some buckling of test section.

[d]Approximate strain range.

[e]Load cycled with high-frequency push-pull fatigue machine.

[f]Approximate number of cycles to failure.

[g]No failure.

[h]Failure outside test section (threads or at buttonhead).

[i]Approximate stress range.

[j]Test-section diameter, 0.18 in.

[k]Hourglass radius, 0.5 in.

[l]Test-section diameter, 0.21 in.

[m]Polished test section.

TABLE IV. - QUANTITATIVE MEASURE OF CYCLIC

STRAIN HARDENING AND SOFTENING

Material	Ratio of stress to produce 1-percent strain after strain cycling to that for the virgin material	
AISI 4130 (hard)	0.60	Cyclic strain softening
AISI 4340 (annealed)	.63	
AISI 4340 (hard)	.64	
1100 aluminum	.68	
AISI 52100	.72	
AISI 4130 (soft)	.75	
Titanium (6Al-4V)	.78	
AM 350 (hard)	.89	
2014-T6 aluminum	.90	
AISI 304 ELC (hard)	1.07	Cyclic strain hardening
Beryllium	1.19	
Inconel X	1.24	
5456-H311 aluminum	1.39	
AISI 310 (annealed)	1.61	
AM 350 (annealed)	2.42	
AISI 304 ELC (annealed)	2.90	

TABLE V. - DIAMETRAL STRAIN RANGE RATINGS OF MATERIALS FOR FATIGUE LIVES OF 100, 3000, AND 100,000 CYCLES

Material	N_f = 100		N_f = 3000		N_f = 100,000	
	$\Delta\epsilon^d$	Rank	$\Delta\epsilon^d$	Rank	$\Delta\epsilon^d$	Rank
1100 aluminum	0.050	1	0.0048	9	0.0010	15
AISI 4130 (soft)	.036	2	.0052	5	.0014	12
Titanium (6Al-4V)	.033	3	.0062	1	.0026	2
AISI 4340 (annealed)	.030	4	.0054	4	.0017	9
AISI 4130 (hard)	.030	4	.0050	8	.0016	11
AISI 310 (annealed)	.029	6	.0056	2	.00138	14
AISI 4340 (hard)	.028	7	.0056	2	.0018	8
Inconel X	.027	8	.0051	7	.0014	12
AISI 304 ELC (hard)	.025	9	.0052	5	.0023	4
AISI 304 ELC (annealed)	.021	10	.0037	15	.0022	5
2014-T6 aluminum	.020	11	.0040	13	.0021	6
5456-H311 aluminum	.019	12	.0039	14	.0017	9
AISI 52100	.014	13	.0046	10	.0020	7
AM 350 (hard)	.012	14	.0042	11	.0026	2
AM 350 (annealed)	.009	15	.0041	12	.0028	1

TABLE VI. - STRESS RANGE RATINGS OF MATERIALS FOR FATIGUE

LIVES OF 100, 3000, AND 100,000 CYCLES

Material	N_f = 100		N_f = 3000		N_f = 100,000		Density, lb/cu in.
	$\Delta\sigma$, ksi	Rank	$\Delta\sigma$, ksi	Rank	$\Delta\sigma$, ksi	Rank	
AM 350 (hard)	510	1	330	1	202	2	0.30
AISI 52100	469	2	321	2	253	1	.30
AM 350 (annealed)	426	3	246	5	148	8	.30
AISI 4340 (hard)	354	4	261	3	189	3	.30
Inconel X	353	5	248	4	155	5	.30
Titanium (6Al-4V)	327	6	241	6	155	6	.16
AISI 304 ELC (hard)	325	7	236	7	145	9	.30
AISI 304 ELC (annealed)	311	8	189	9	105	11	.30
AISI 4130 (hard)	293	9	223	8	178	4	.30
AISI 4130 (soft)	252	10	173	10	150	7	.30
AISI 4340 (annealed)	213	11	143	11	112	10	.30
AISI 310 (annealed)	213	12	120	13	72	12	.30
2014-T6 aluminum	144	13	123	12	72	13	.10
5456-H311 aluminum	122	14	95	14	58	15	.10
Beryllium	102	15	81	15	64	14	.07
1100 aluminum	29	16	18	16	15	16	.10

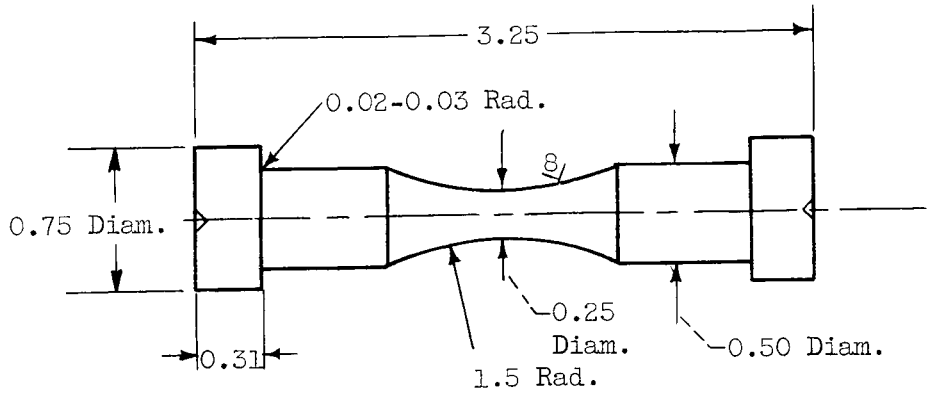

(a) Buttonhead fatigue specimen.

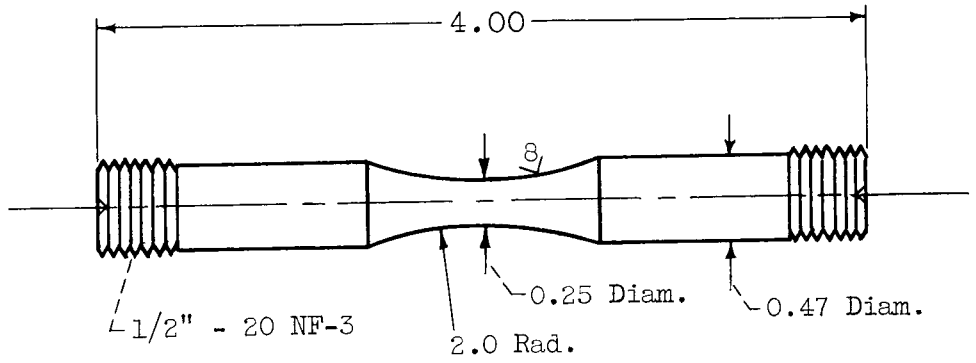

(b) Threaded-head fatigue specimen.

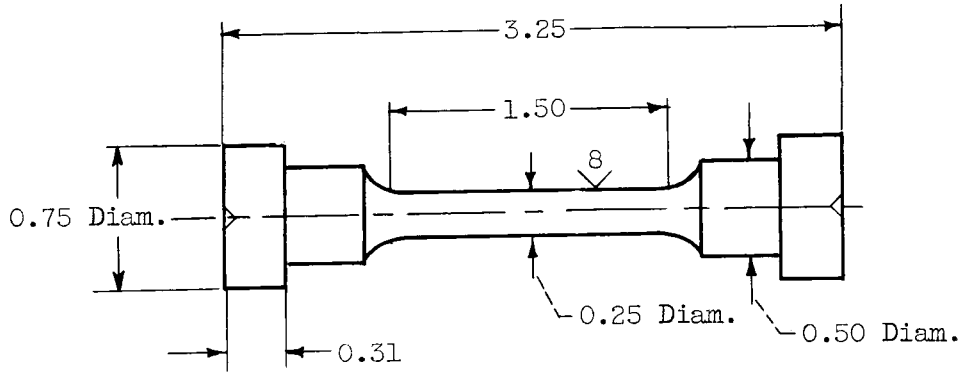

(c) Specimen used for moduli determinations and beryllium fatigue tests.

Figure 1. - Test specimen configurations. (All dimensions in inches.)

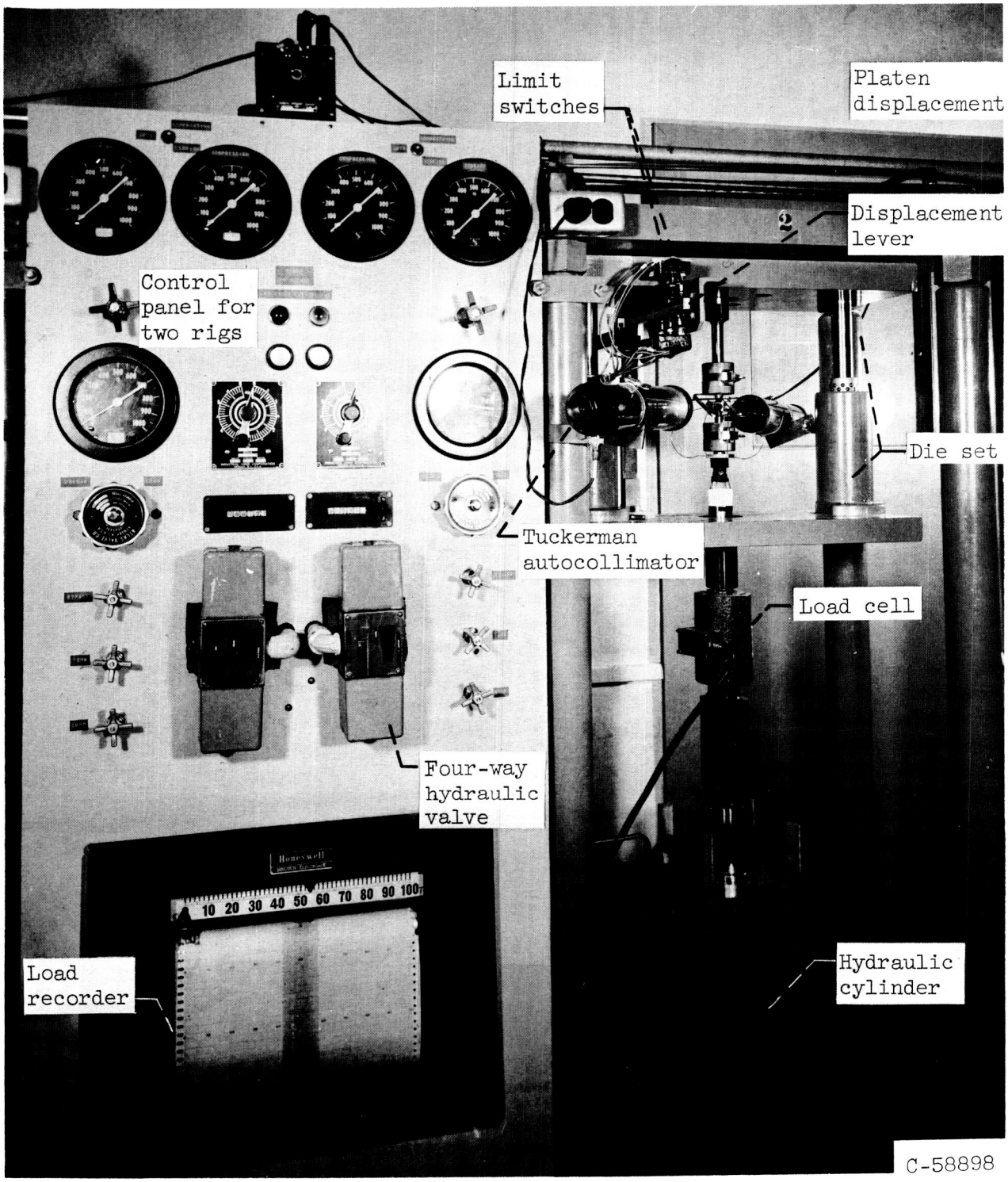

Figure 2. - Low-frequency fatigue machine.

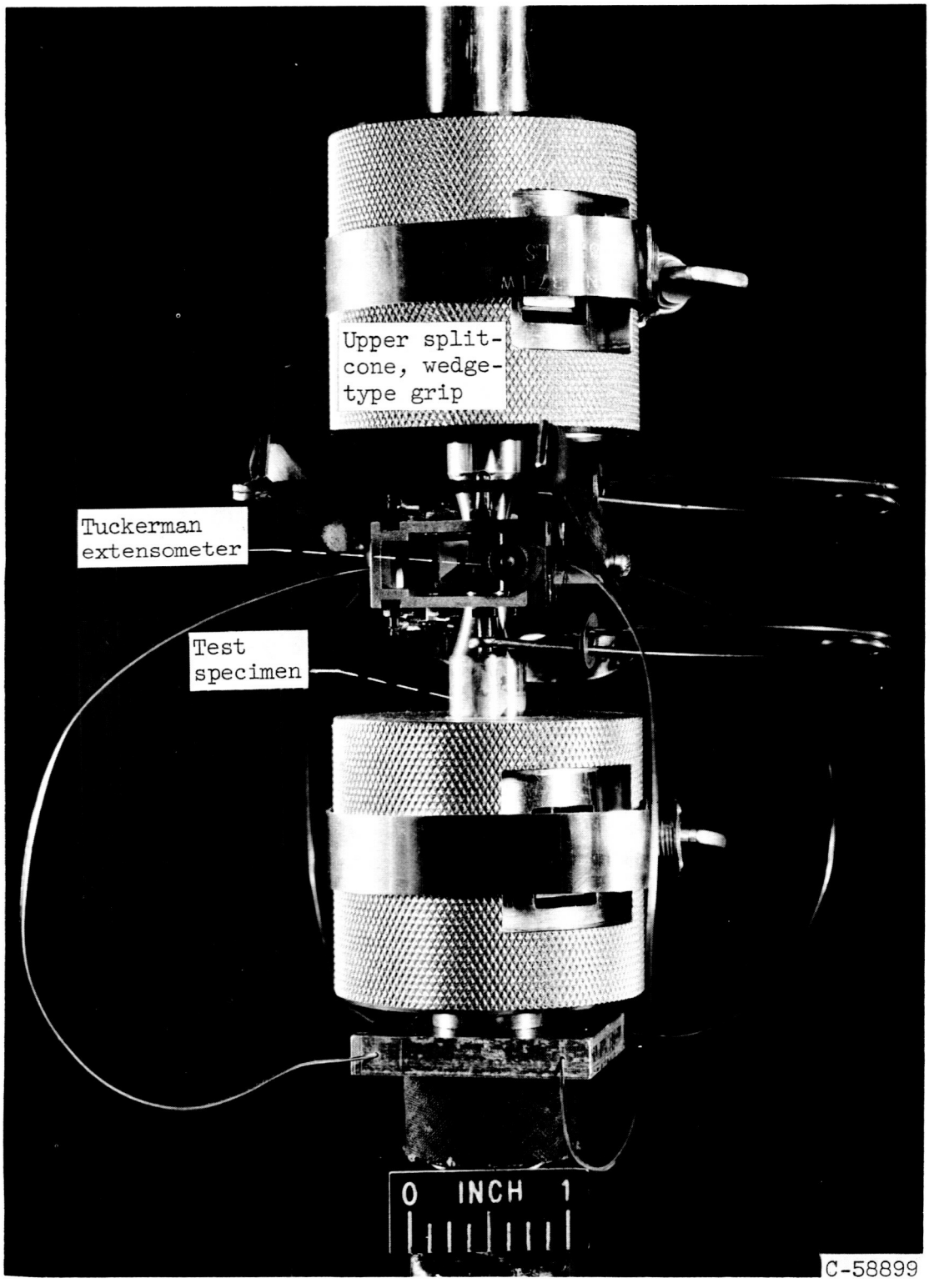

(a) Horizontal view of assembly during test.

Figure 3. - Diametral strain-gage fixture.

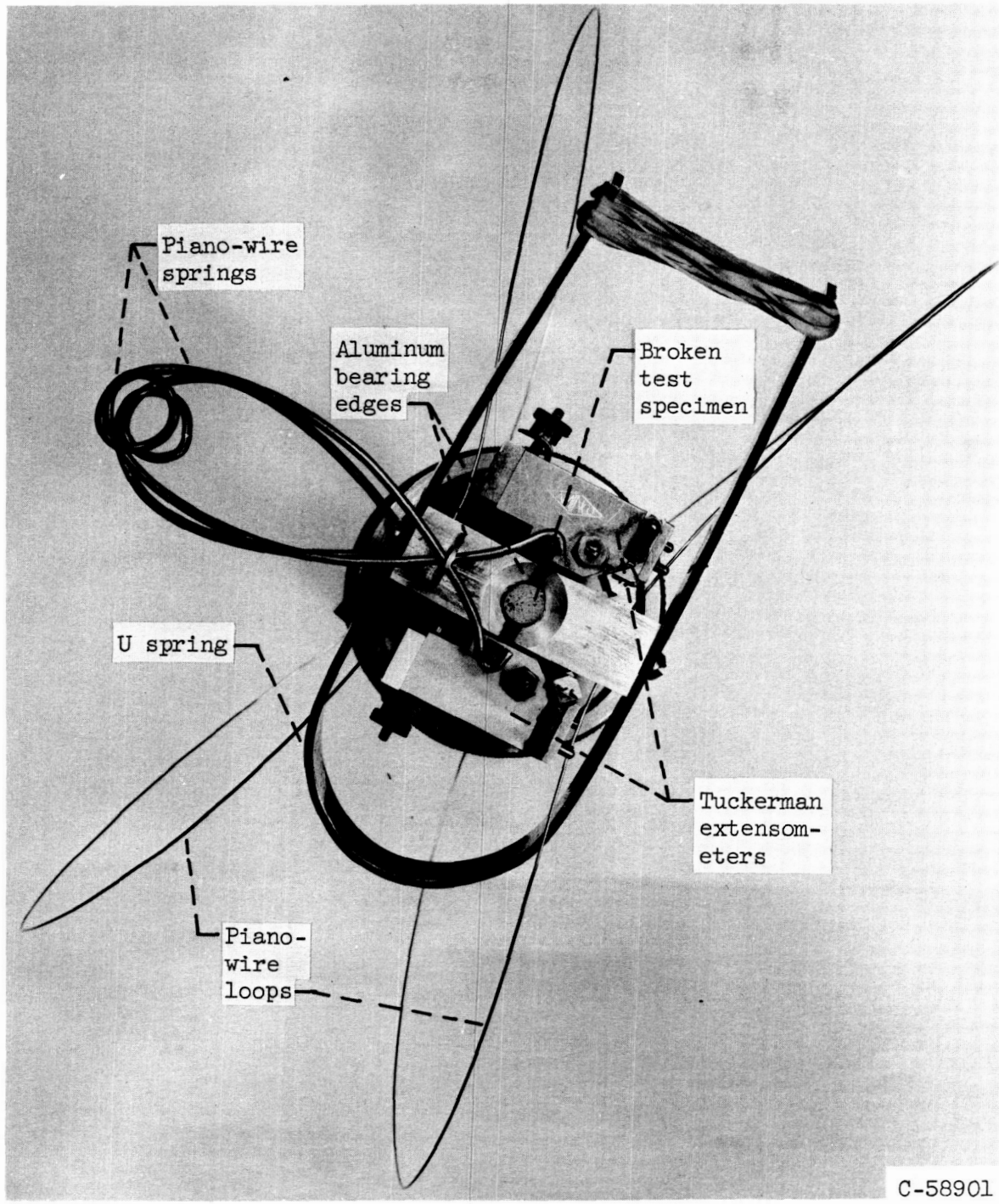

(b) Vertical view of assembly after specimen failure.

Figure 3. - Concluded. Diametral strain-gage fixture.

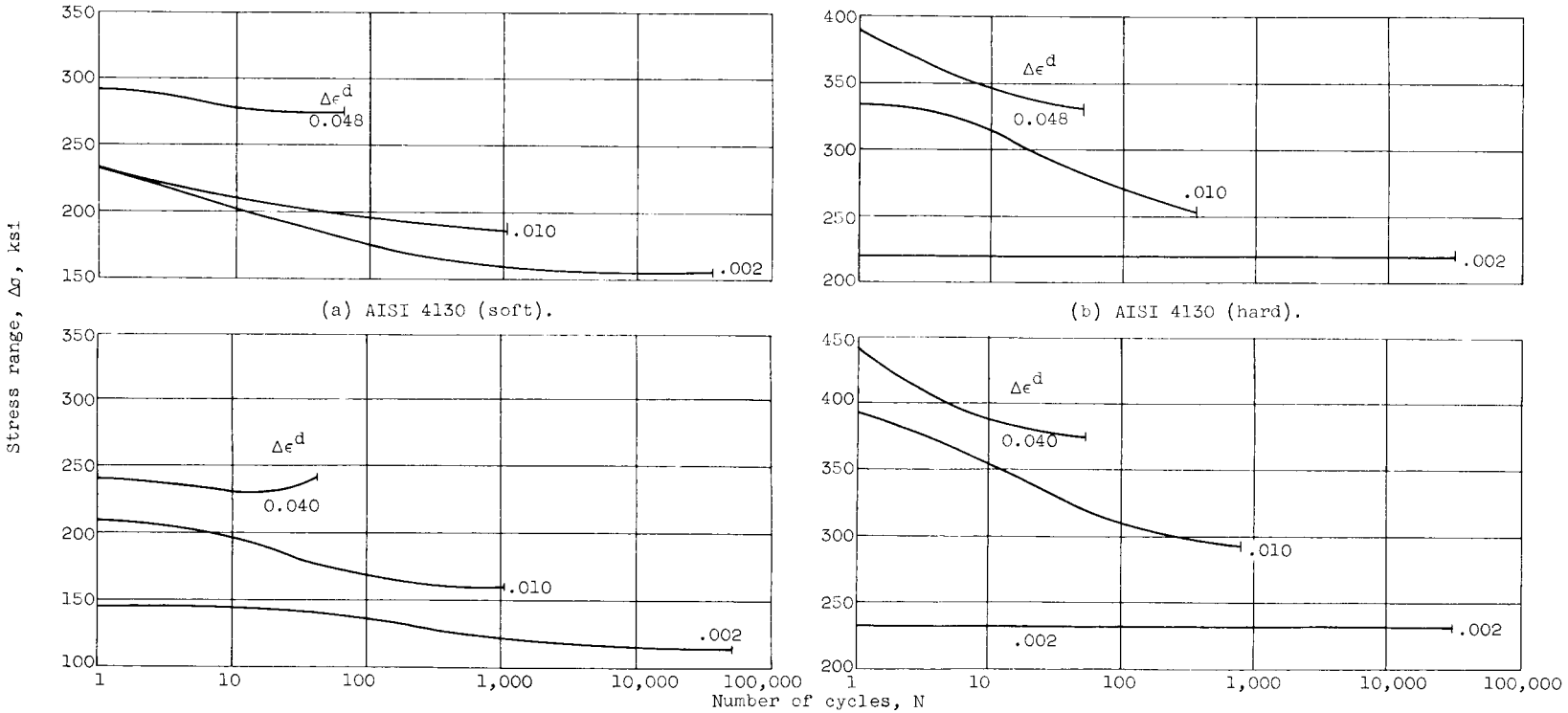

(a) AISI 4130 (soft).

(b) AISI 4130 (hard).

(c) AISI 4340 (annealed).

(d) AISI 4340 (hard).

Figure 4. - Variation of stress range with cycles for strain cycling about a zero mean strain.

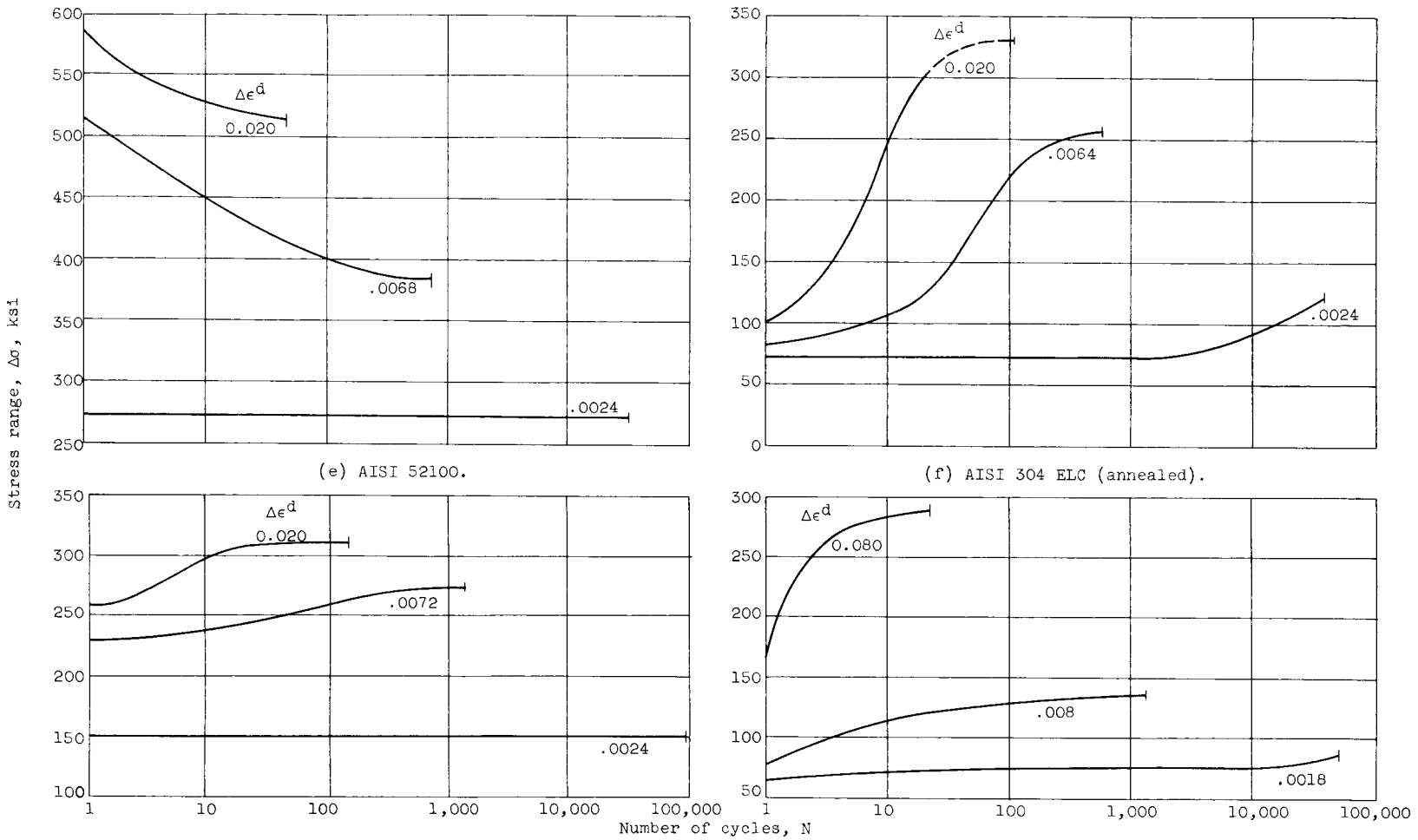

Figure 4. - Continued. Variation of stress range with cycles for strain cycling about a zero mean strain.

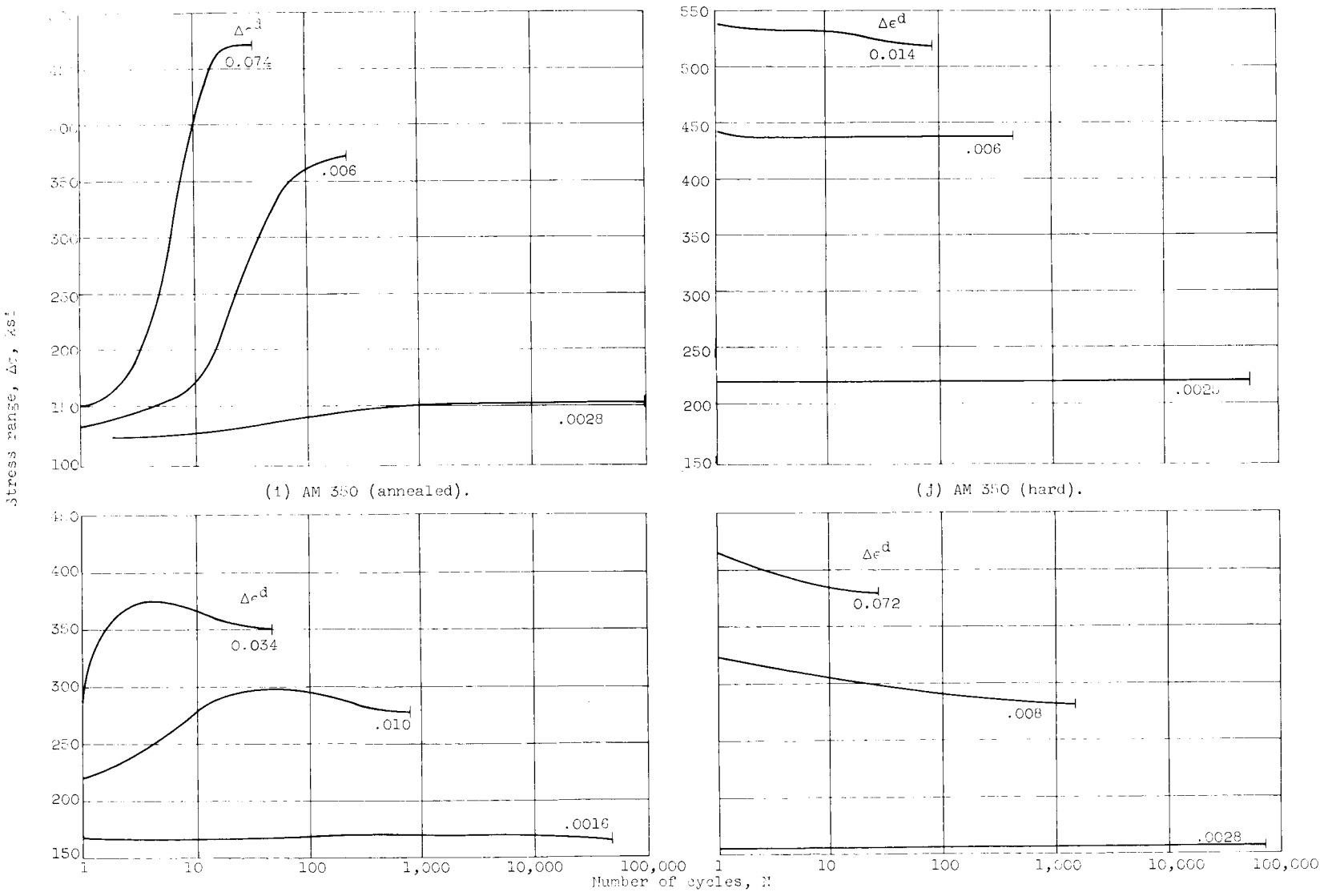

Figure 4. - Continued. Variation of stress range with cycles for strain cycling about a zero mean strain.

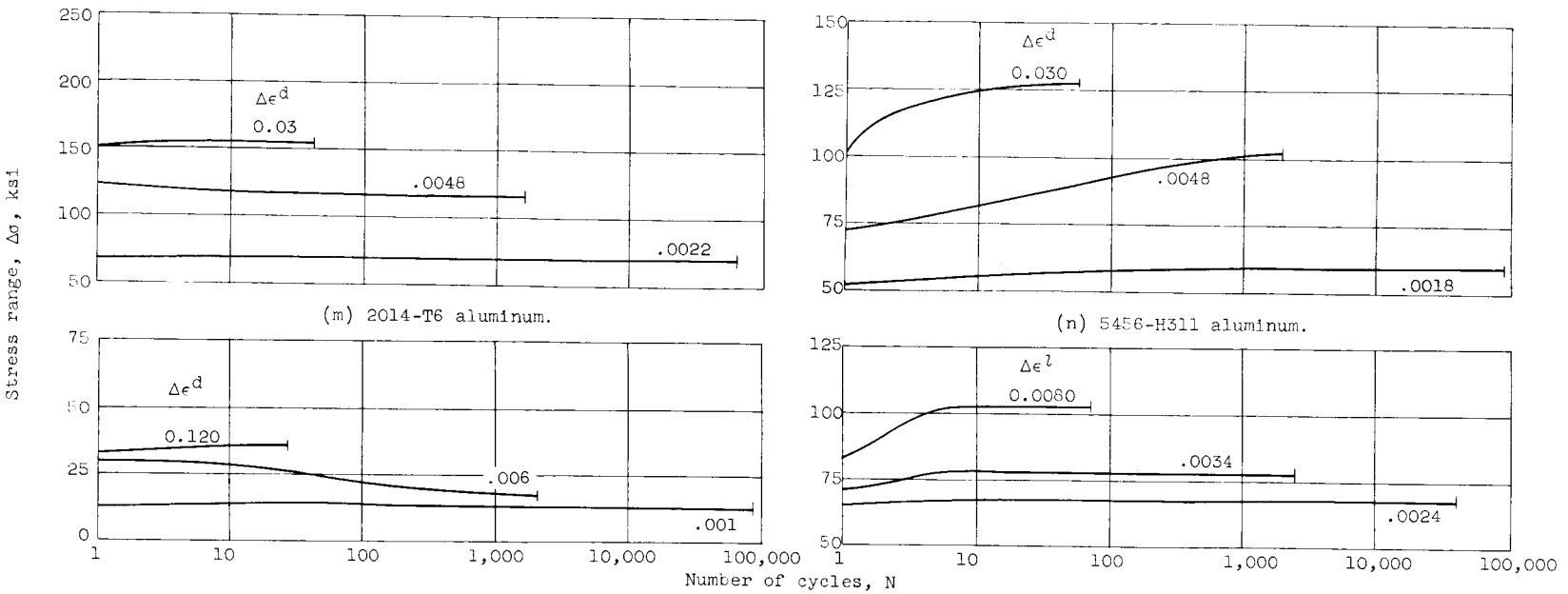

Figure 4. - Concluded. Variation of stress range with cycles for strain cycling about a zero mean strain.

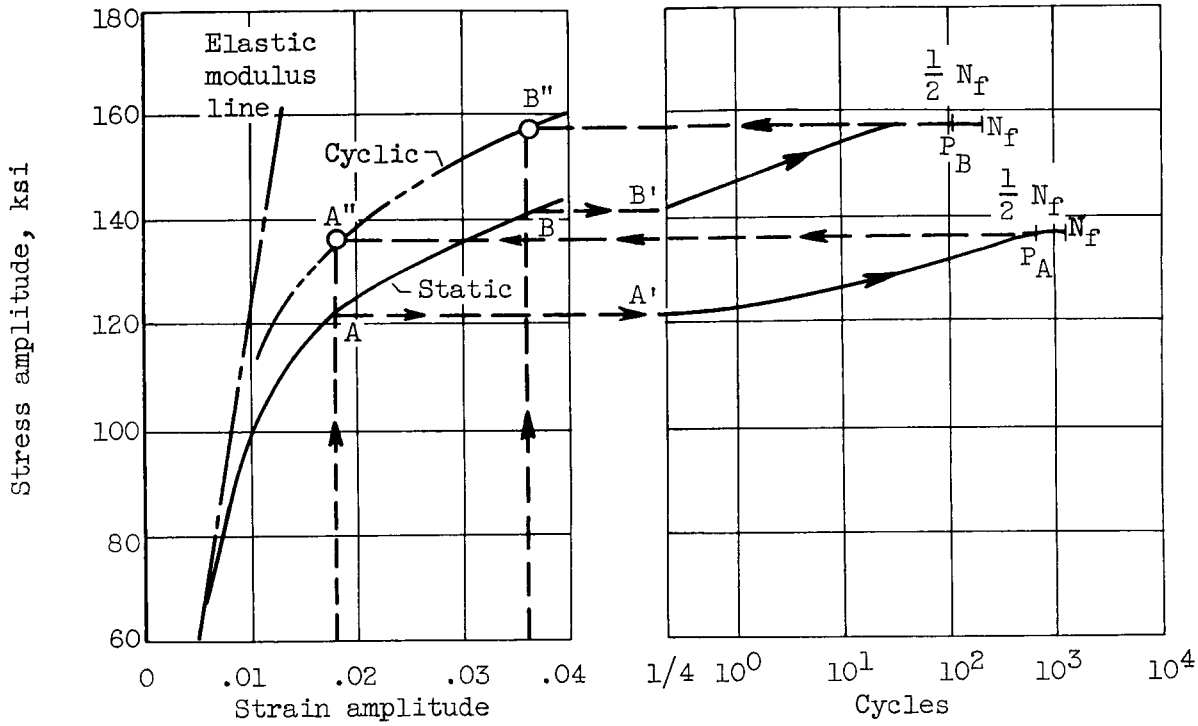

(a) Static and cyclic stress-strain characteristics.

(b) Stress range as a function of applied cycles, logarithmic scale for cycles.

Figure 5. - Static and cyclic stress characteristics of a hypothetical cyclic strain hardening material.

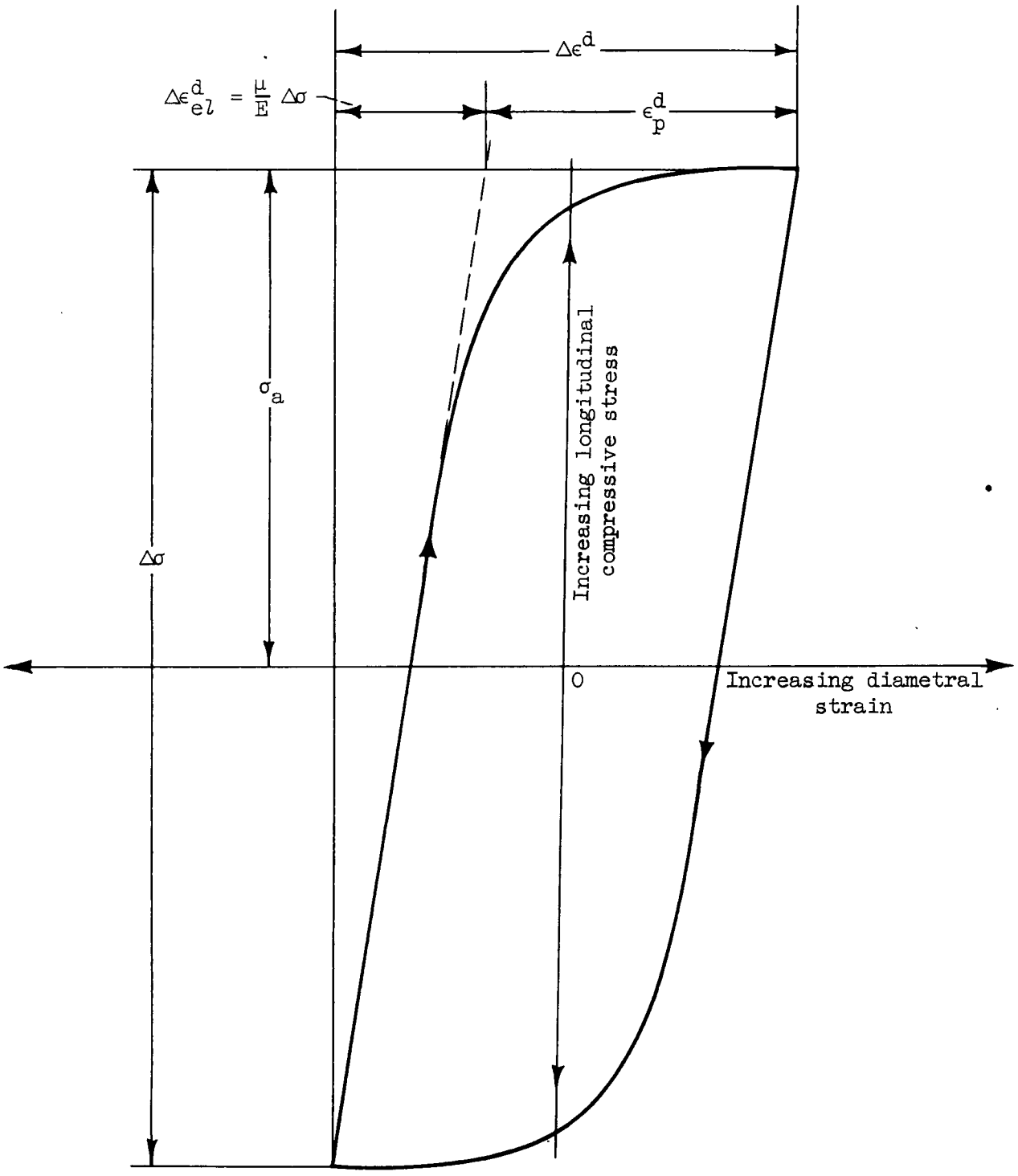

Figure 6. - Hypothetical axial stress - diametral strain relation during strain cycling in which mean strain is zero.

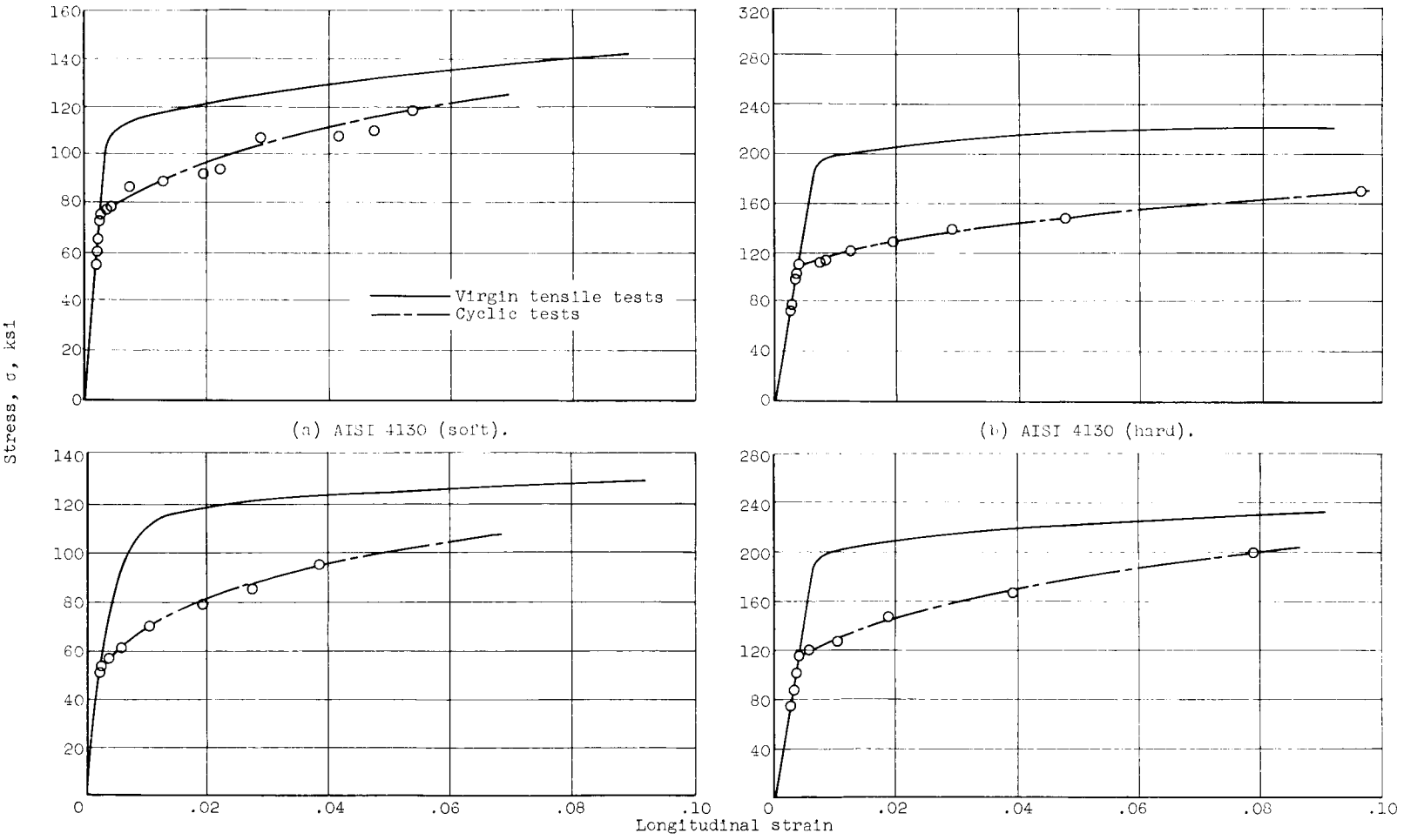

(a) AISI 4130 (soft).

(b) AISI 4130 (hard).

(c) AISI 4340 (annealed).

(d) AISI 4340 (hard).

Figure 7. - Comparison of cyclic and virgin tensile stress-strain curves.

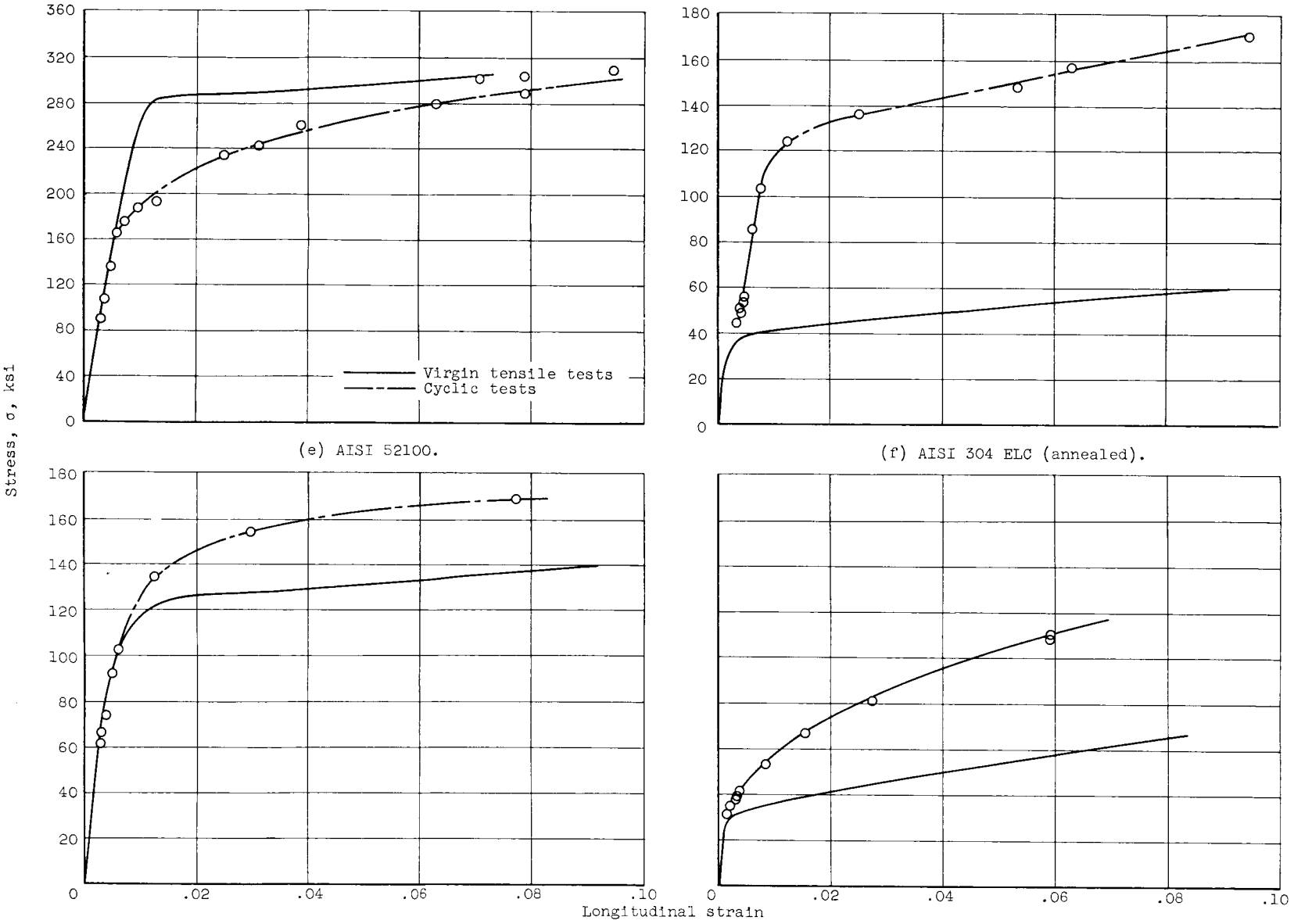

(e) AISI 52100.

(f) AISI 304 ELC (annealed).

(g) AISI 304 ELC (hard).

(h) AISI 310 (annealed).

Figure 7. - Continued. Comparison of cyclic and virgin tensile stress-strain curves.

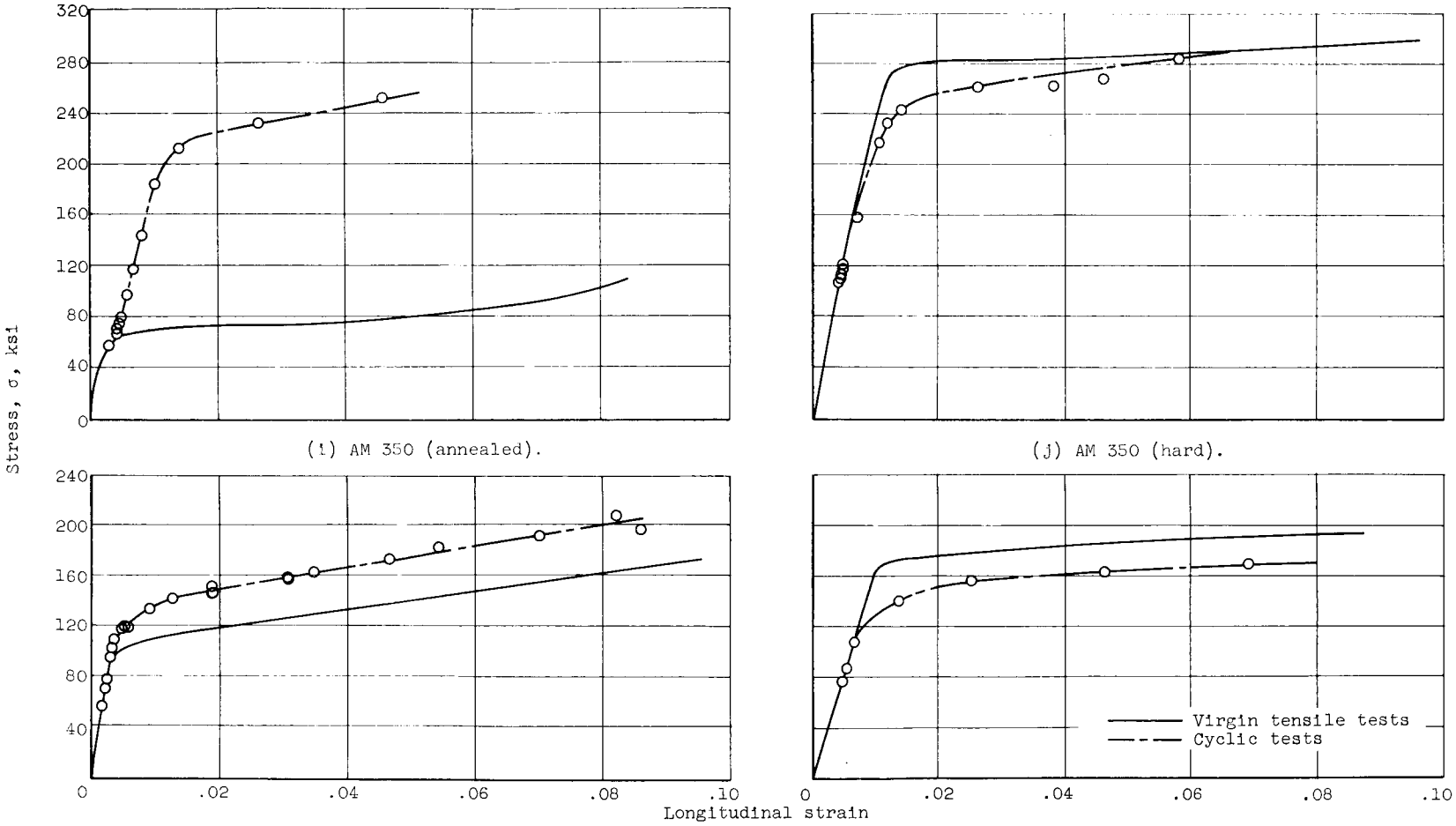

(i) AM 350 (annealed).

(j) AM 350 (hard).

(k) Inconel X.

(l) Titanium (6Al-4V).

Figure 7. - Continued. Comparison of cyclic and virgin tensile stress-strain curves.

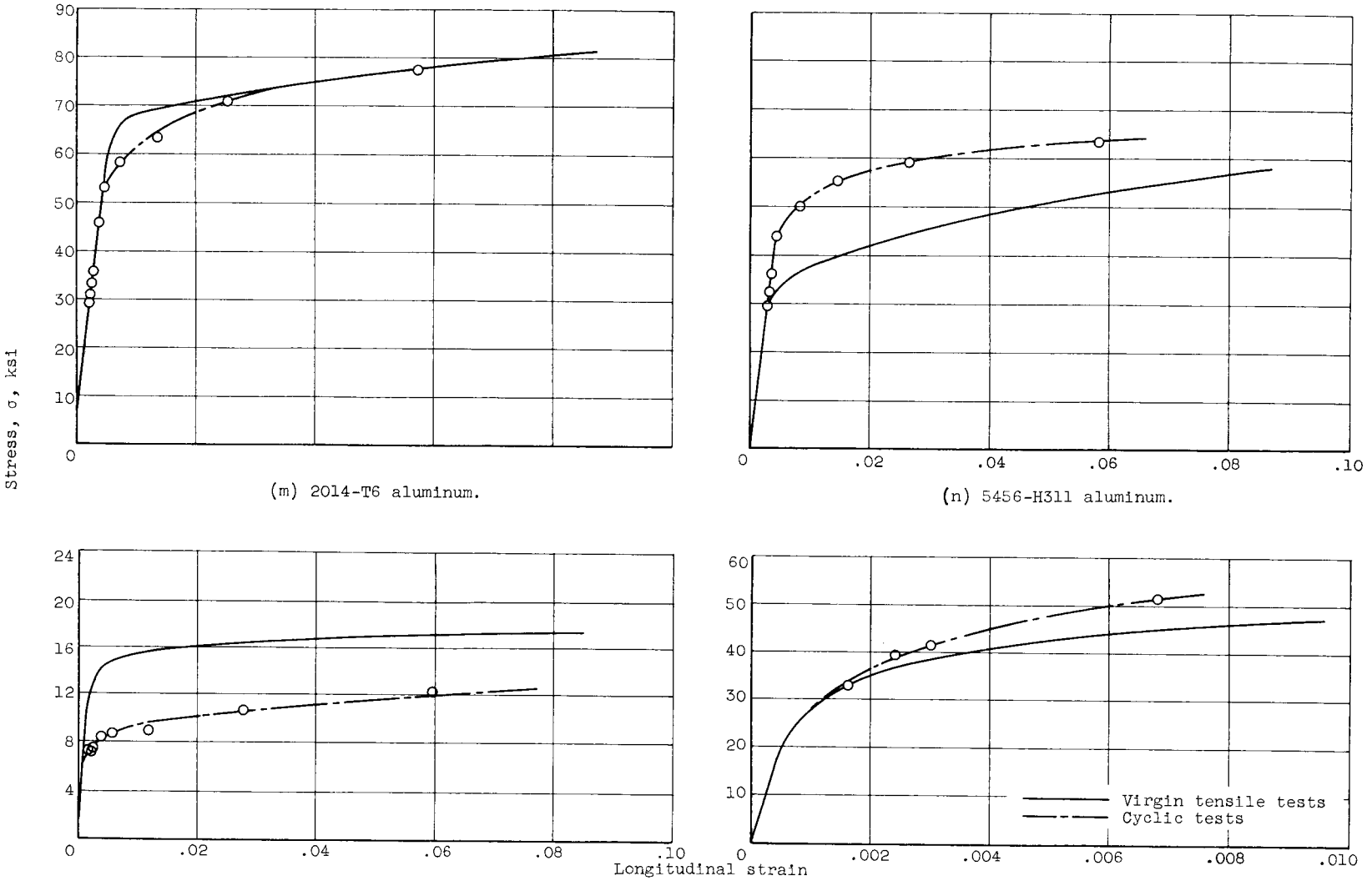

(m) 2014-T6 aluminum.

(n) 5456-H311 aluminum.

(o) 1100 aluminum.

(p) Beryllium.

Figure 7. - Concluded. Comparison of cyclic and virgin tensile stress-strain curves.

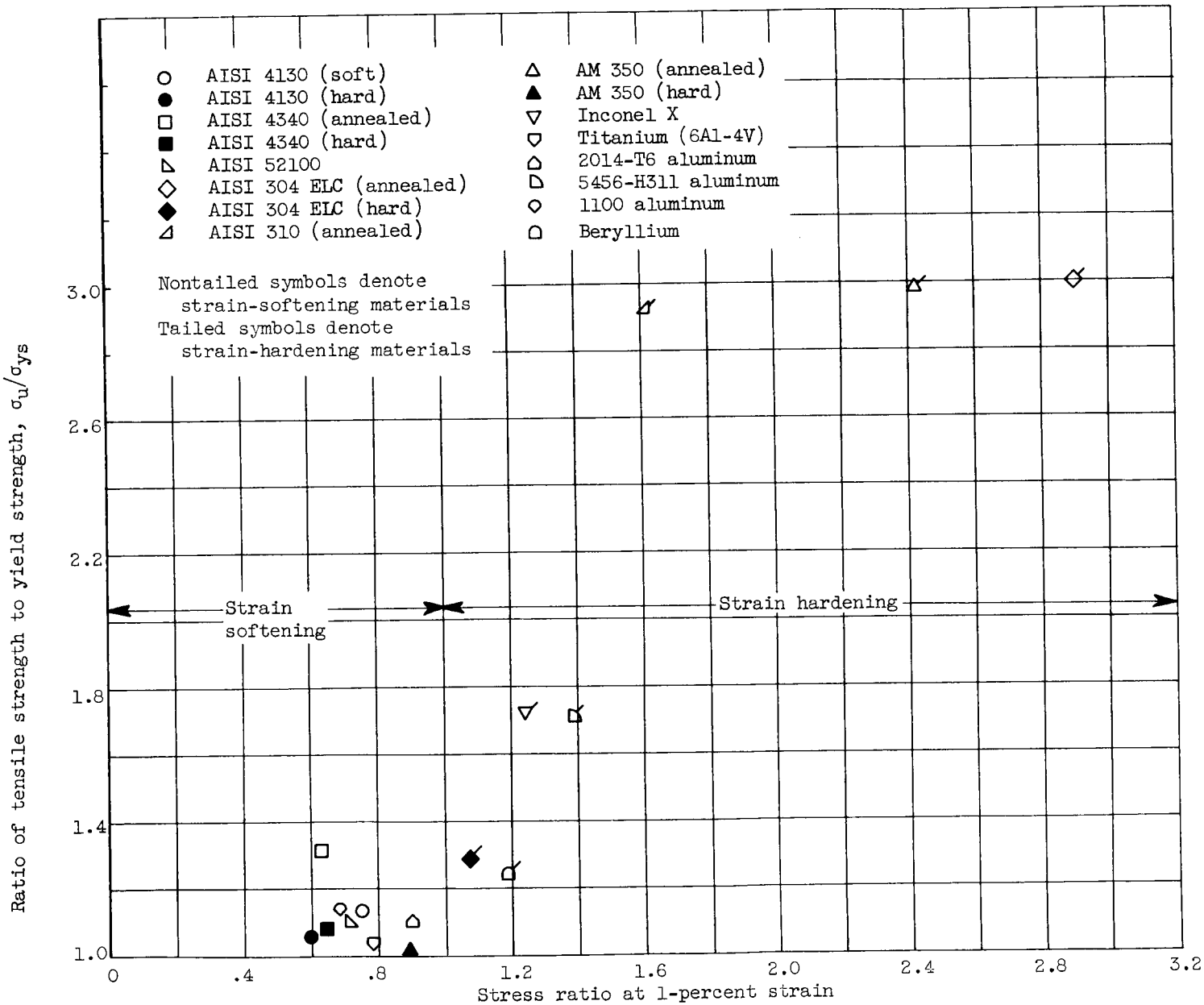

Figure 8. - Comparison of stress ratio at 1-percent strain with virgin tensile properties.

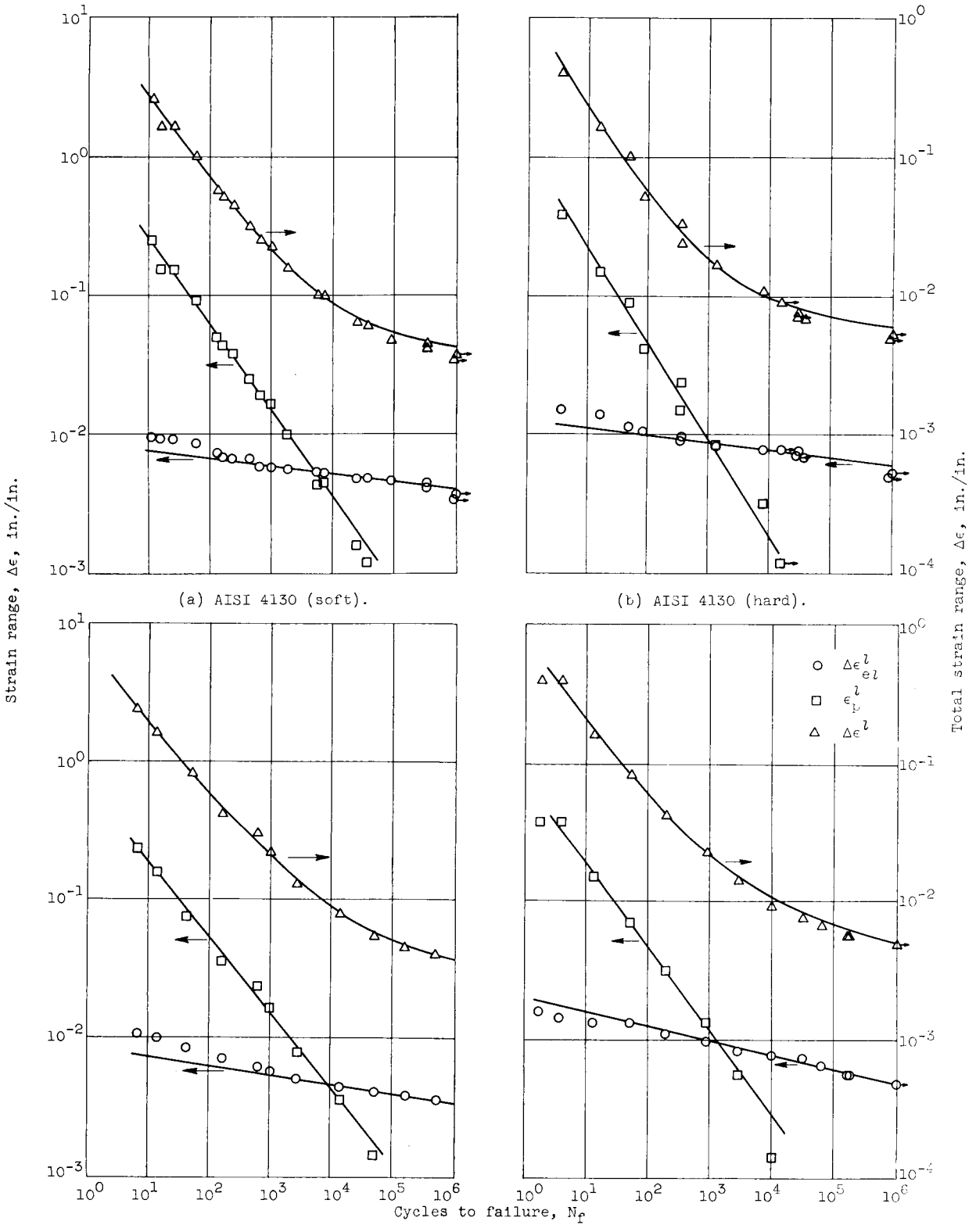

(a) AISI 4130 (soft).

(b) AISI 4130 (hard).

(c) AISI 4340 (annealed).

(d) AISI 4340 (hard).

Figure 9. - Elastic, plastic, and total strain range variations with cyclic life.

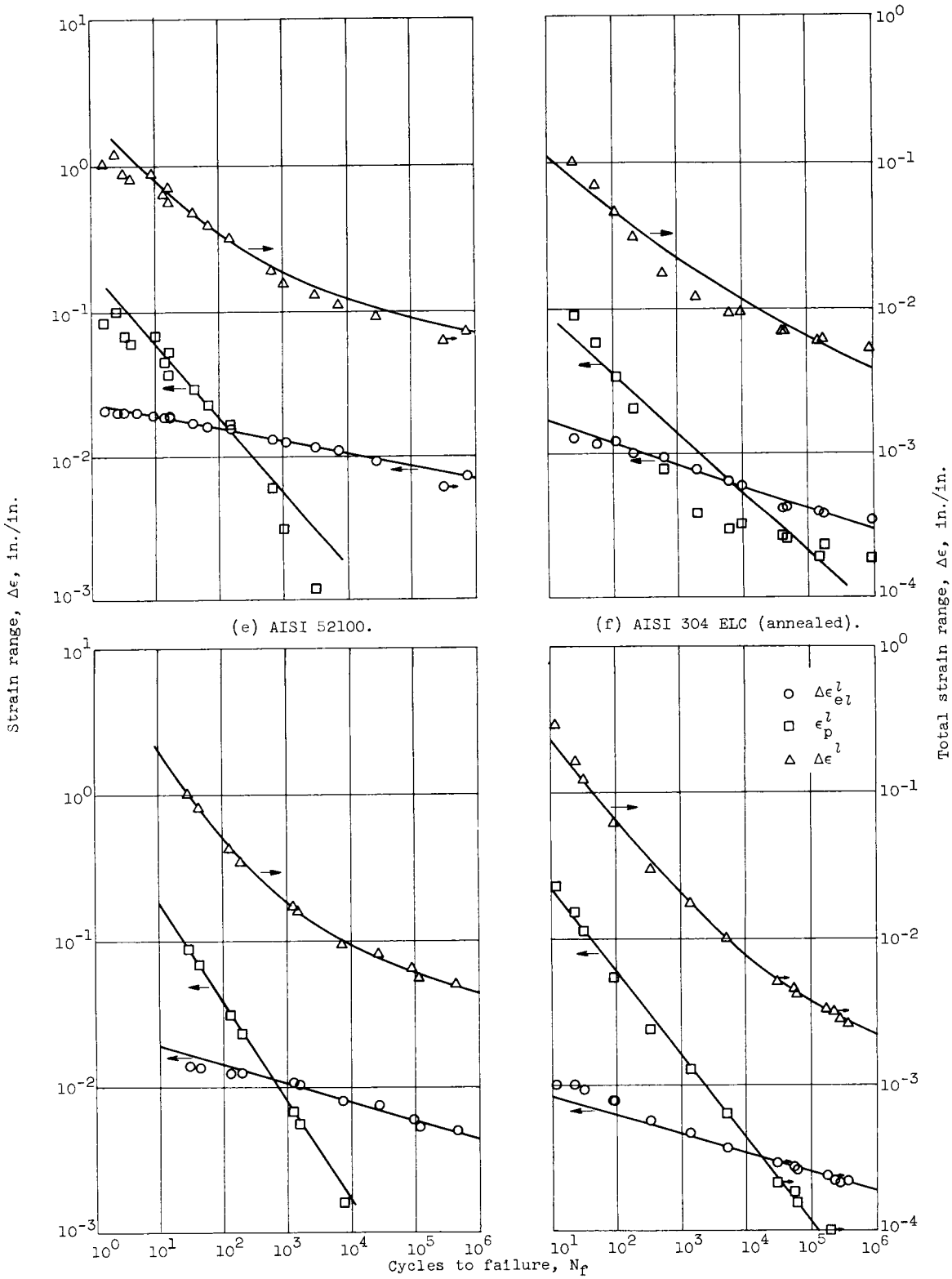

(e) AISI 52100.

(f) AISI 304 ELC (annealed).

(g) AISI 304 ELC (hard).

(h) AISI 310 (annealed).

Figure 9. - Continued. Elastic, plastic, and total strain range variations with cyclic life.

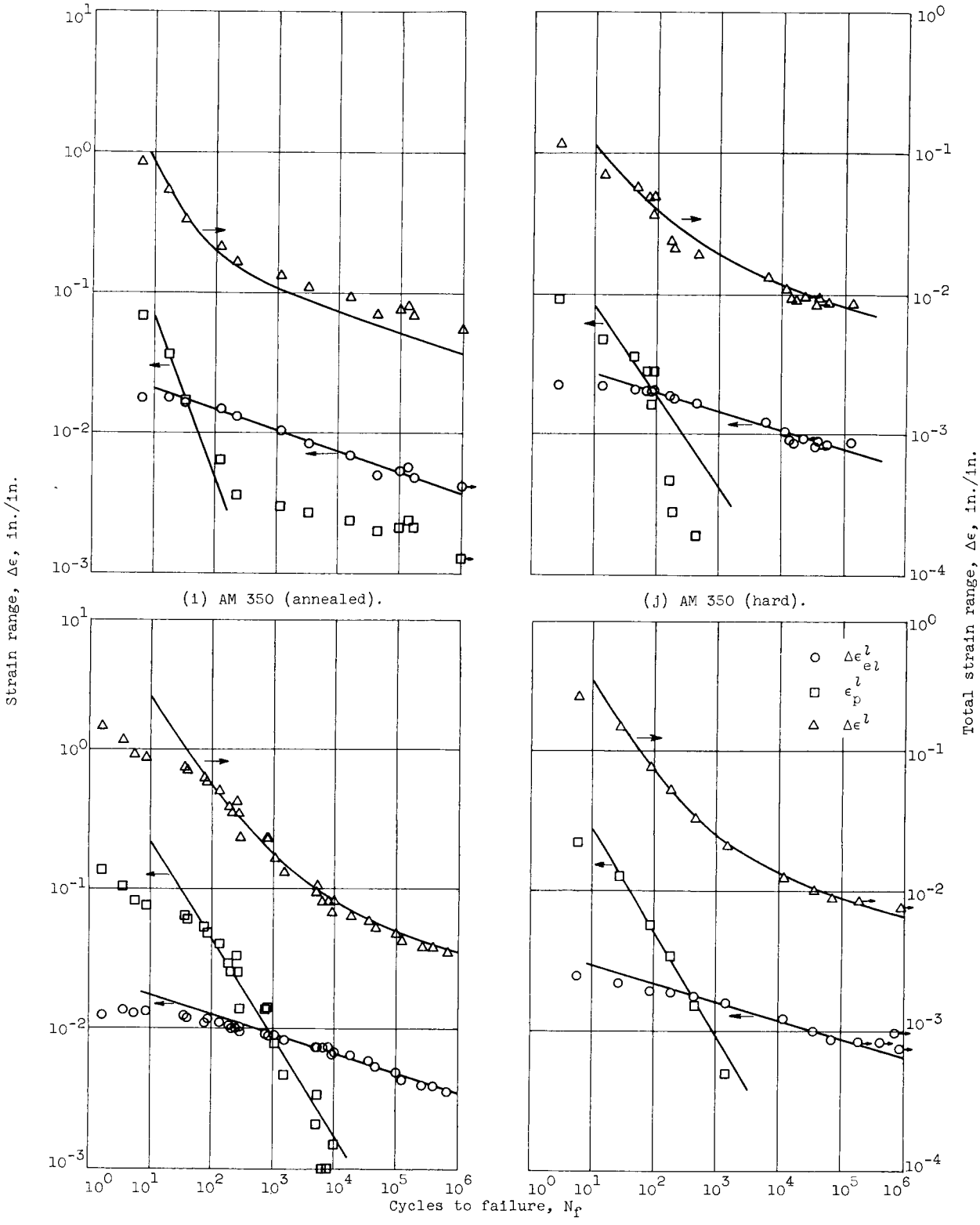

(i) AM 350 (annealed).

(j) AM 350 (hard).

(κ) Inconel X.

(l) Titanium (6Al-4V).

Figure 9. - Continued. Elastic, plastic, and total strain range variations with cyclic life.

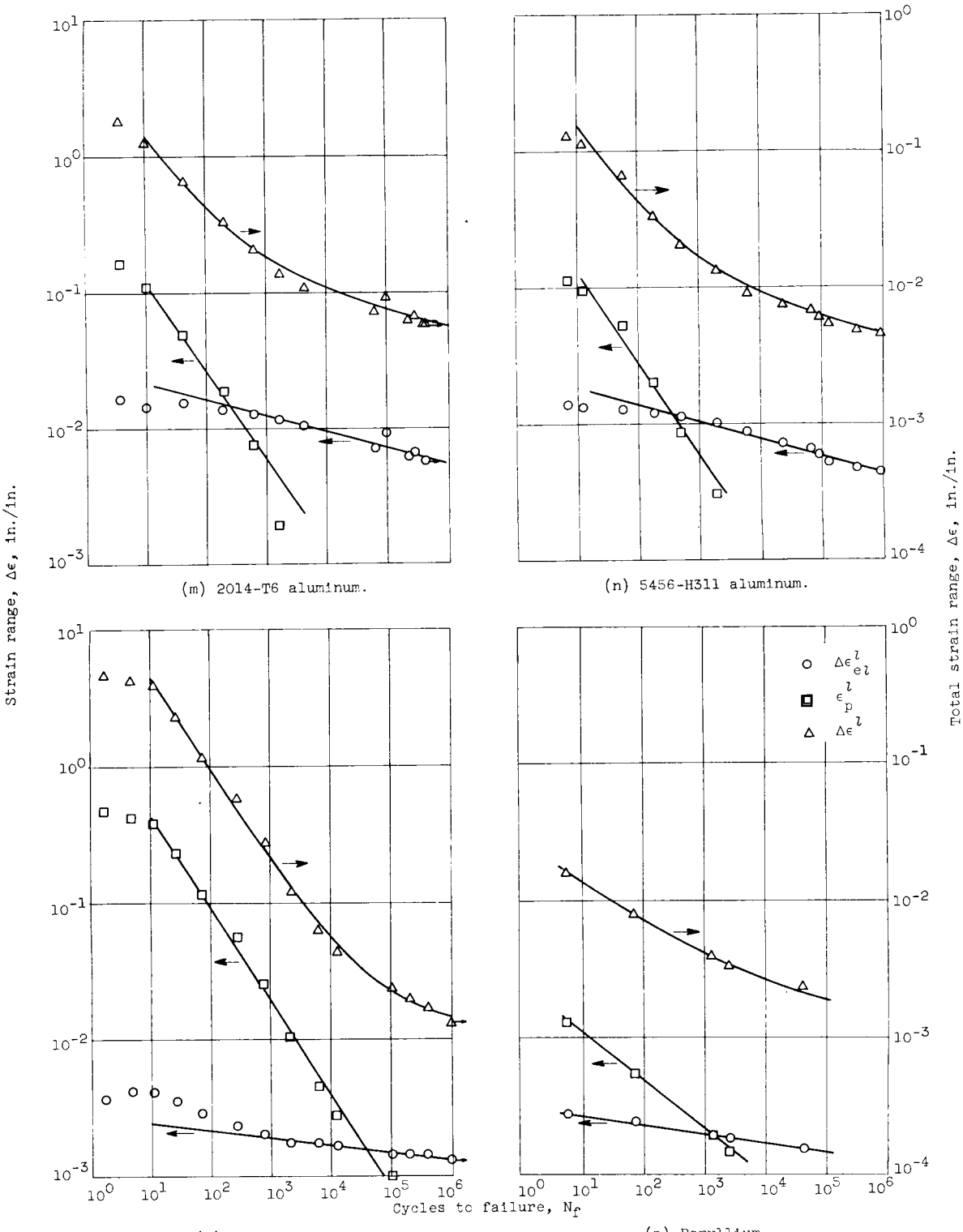

(m) 2014-T6 aluminum.

(n) 5456-H311 aluminum.

(o) 1100 aluminum.

(p) Beryllium.

Figure 9. - Concluded. Elastic, plastic, and total strain range variations with cyclic life.

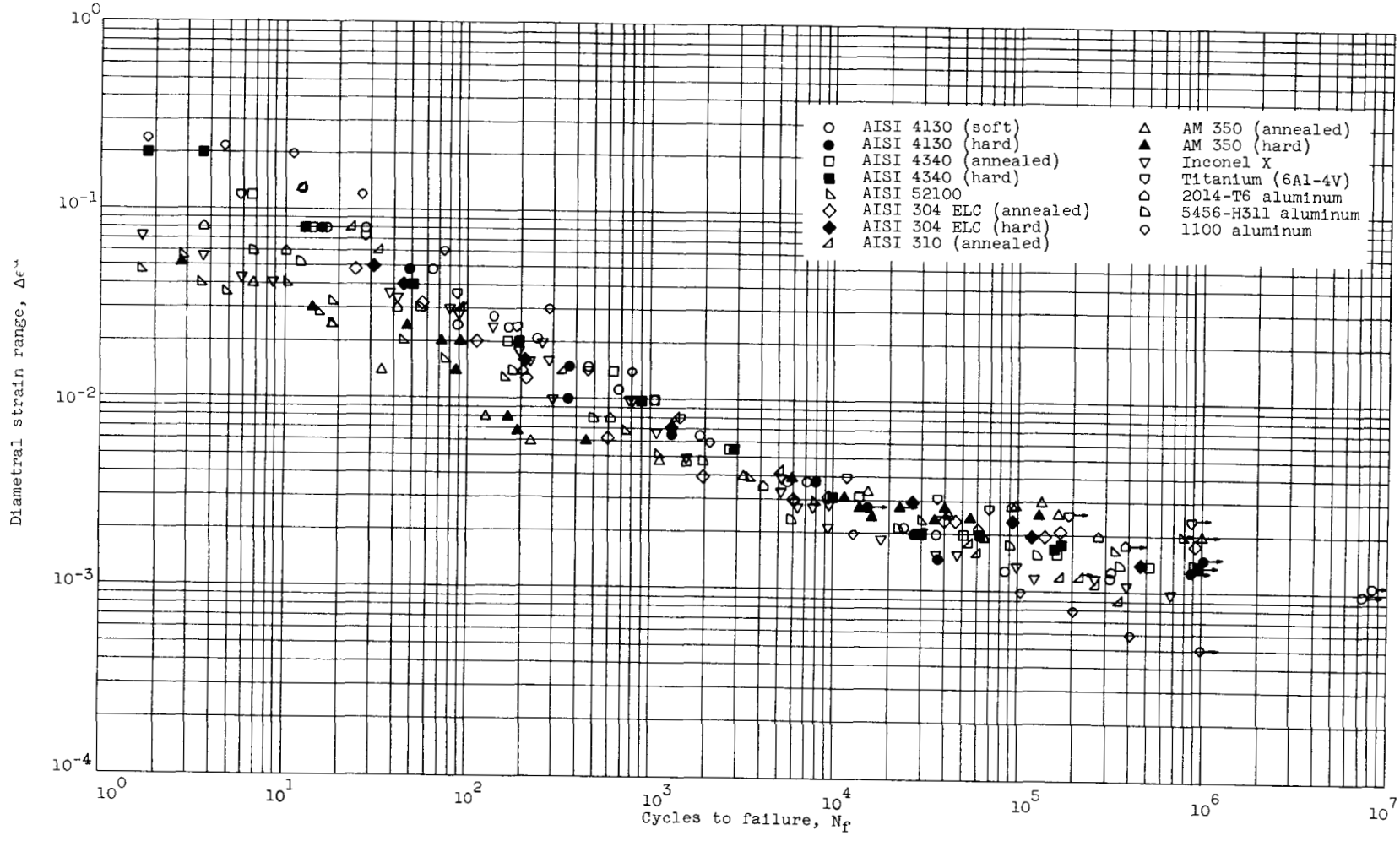

Figure 10. - Effect of diametral strain range on fatigue life.

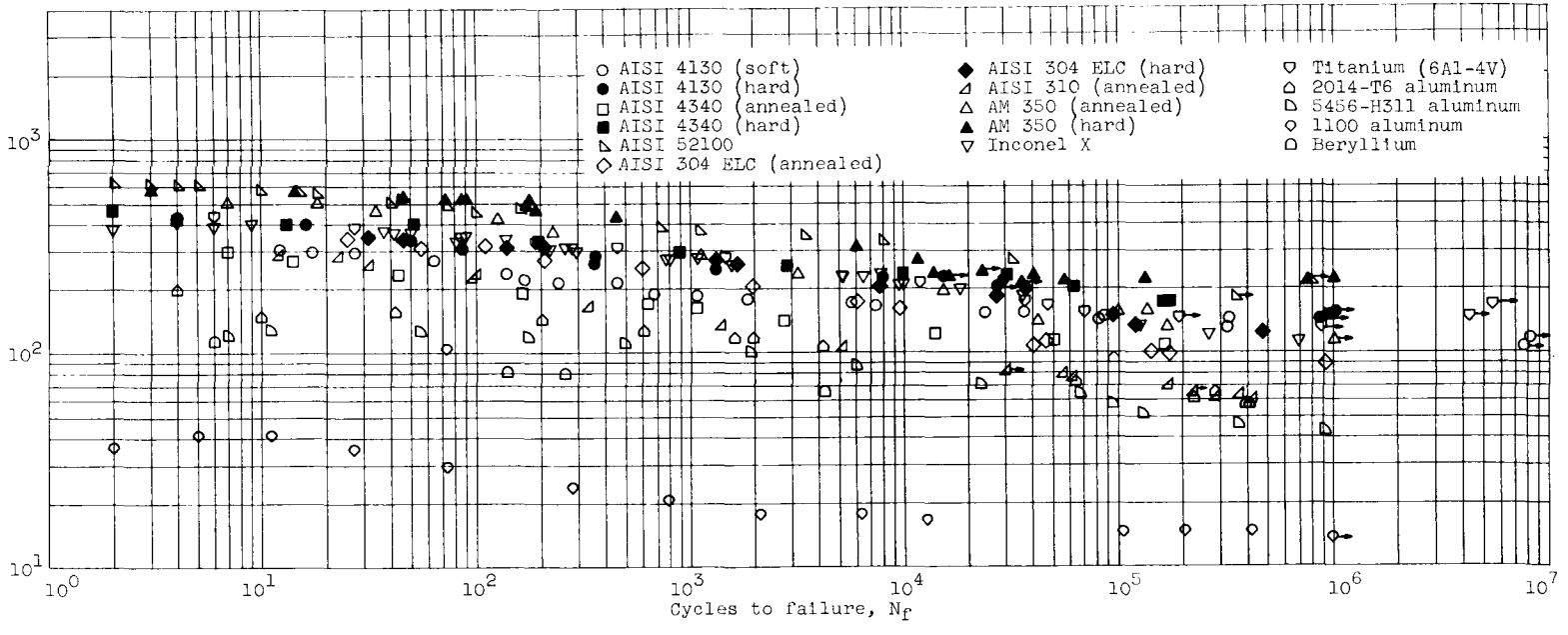

Figure 11. - Variation of stress range at $\frac{1}{2} N_f$ with fatigue life for constant strain range cycling.

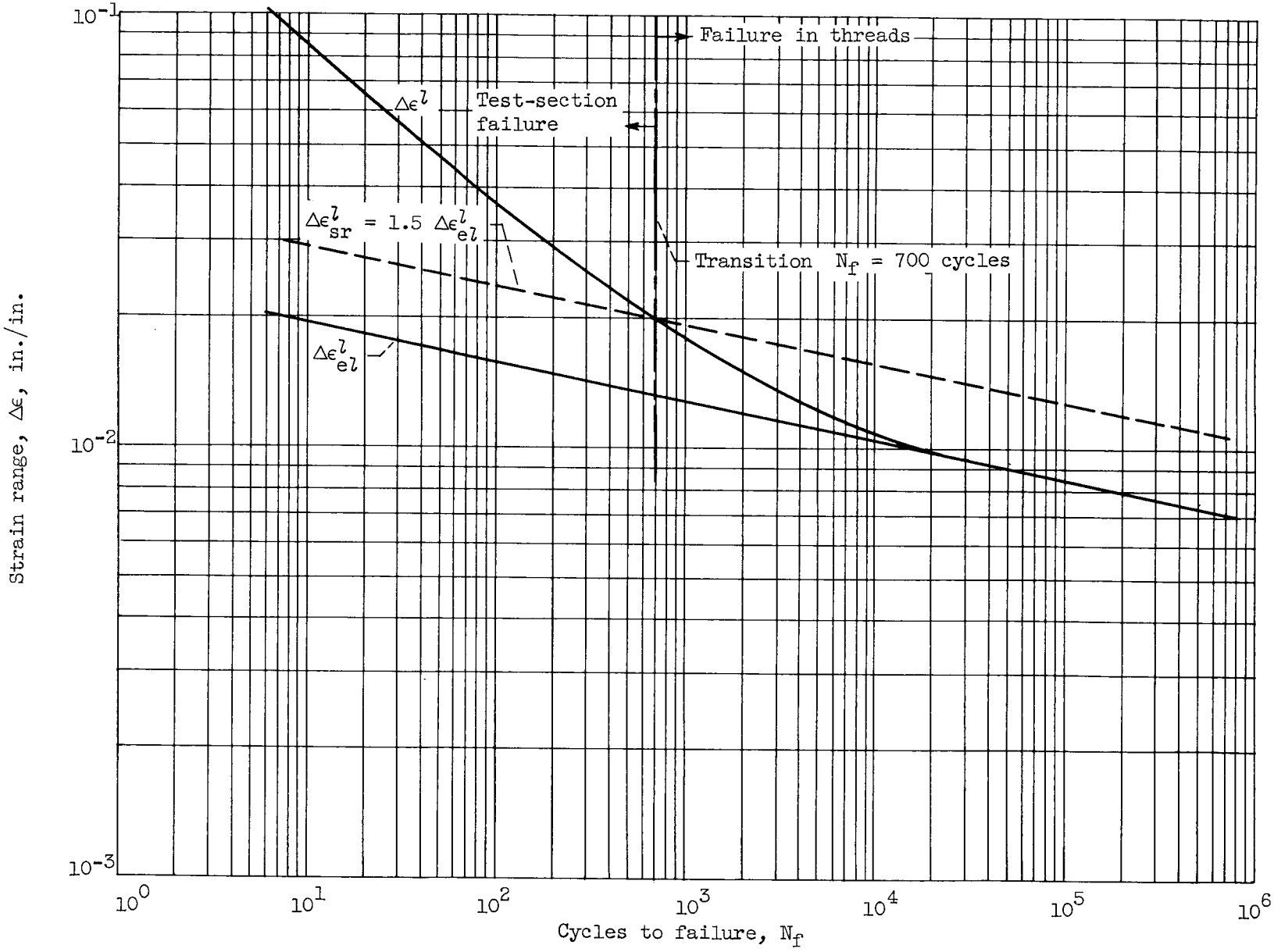

Figure 12. - Graphical illustration of failure transition in test specimen based upon strain-life relations for AISI 52100 steel and an assumed stress concentration factor.

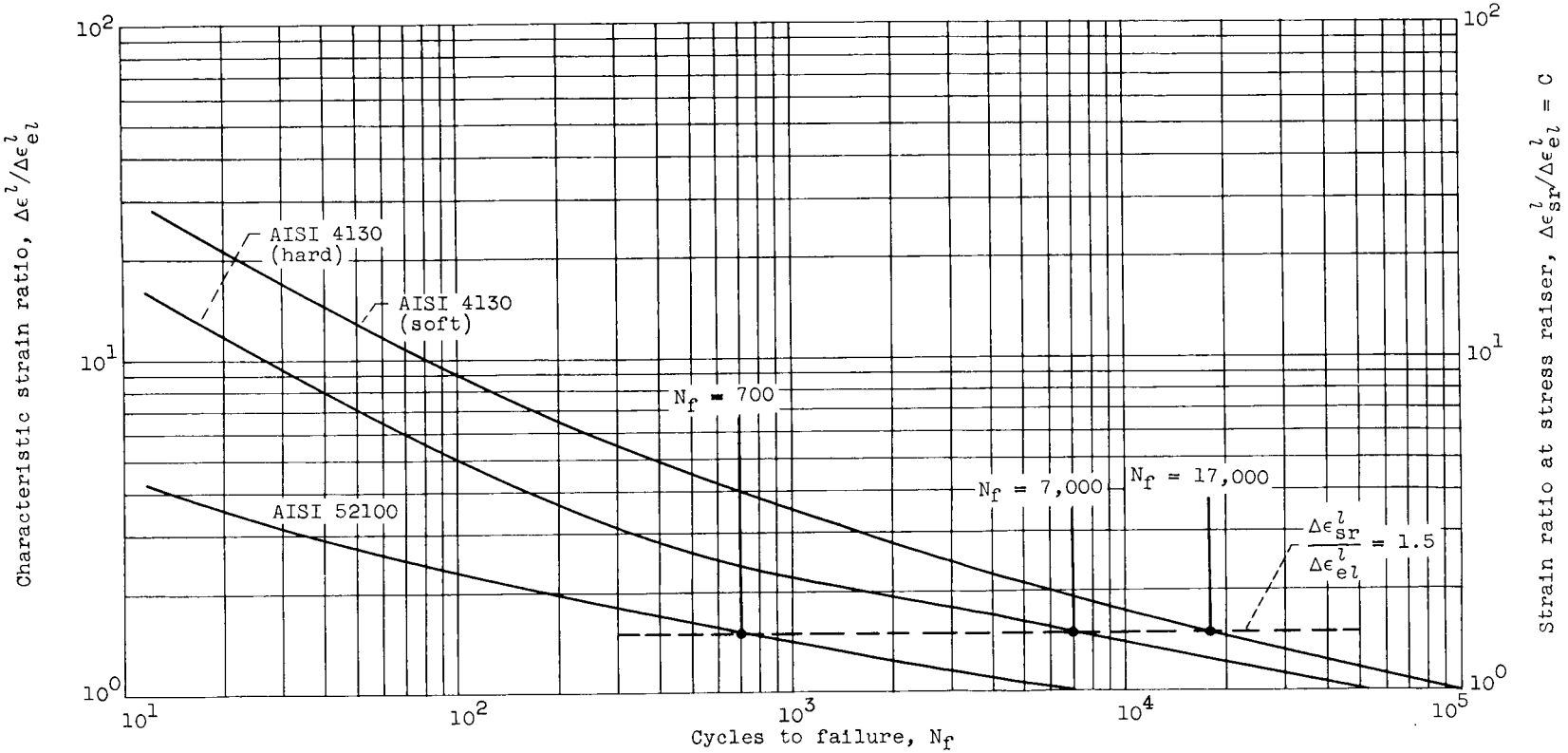

Figure 13. - Relative notch sensitivity behavior of threaded specimens as indicated by strain ratio against life curves.

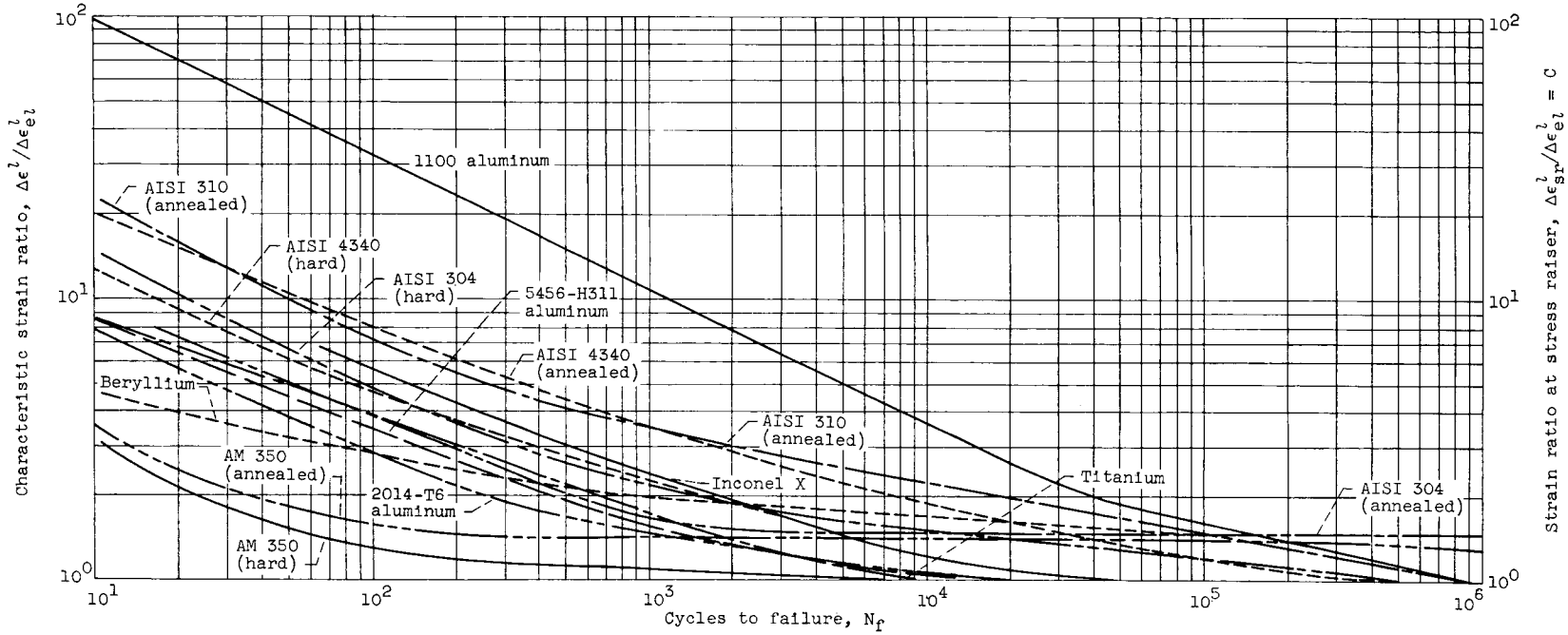

Figure 14. - Relative notch sensitivity behavior of buttonhead specimen as indicated by strain ratio against life curves.

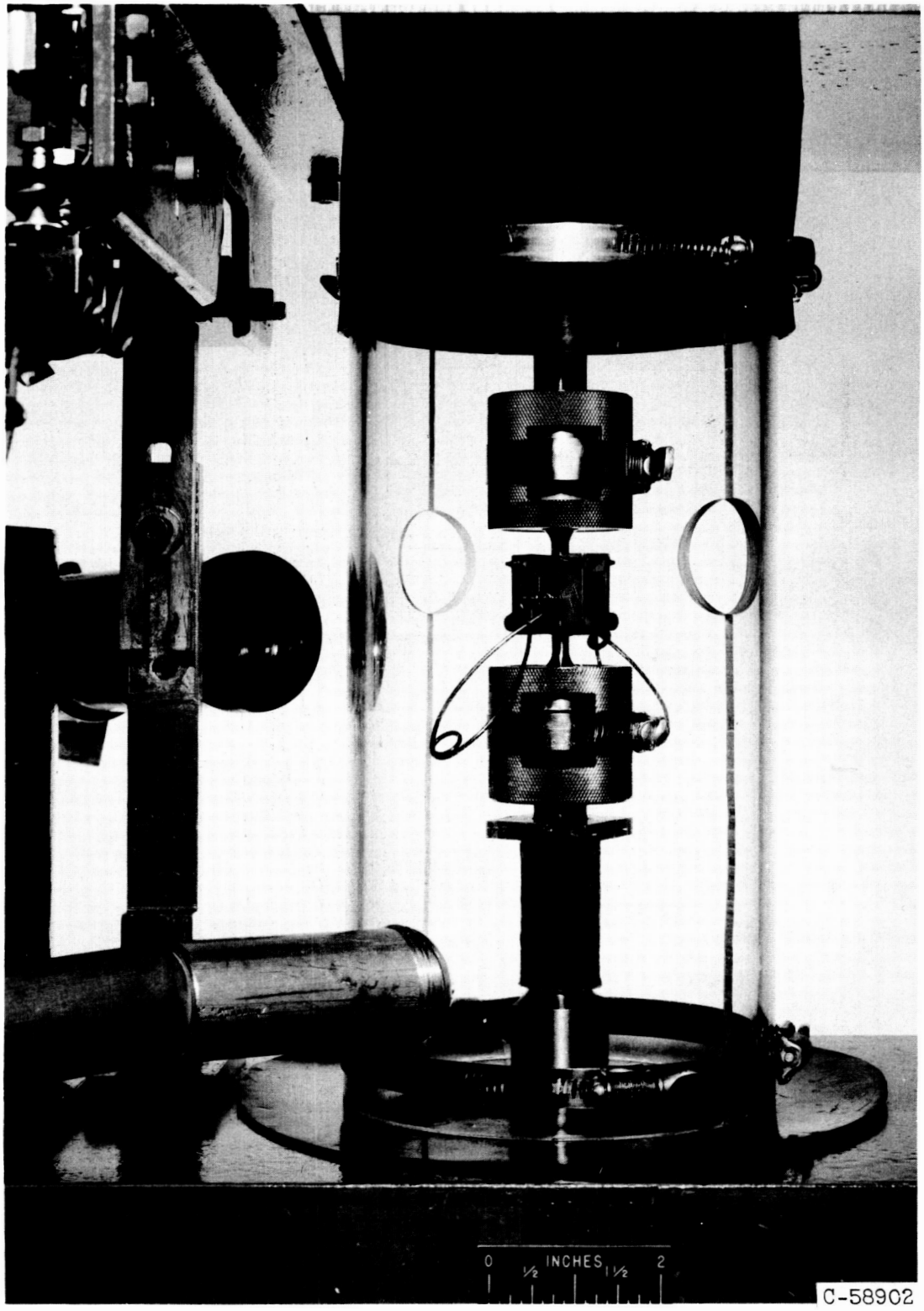

Figure 15. - Protective assembly for testing beryllium.